Design and Optimization of a Wind Powered Ice Fishing Jigging Mechanism

A Major Qualifying Project submitted to the faculty

of Worcester Polytechnic Institute in partial fulfillment of the

requirements for the Degree of Bachelor of Science.

Submitted By:

Austin Brais

Daryn Russo

Tyler Tilbe

Submitted To:

Advisors: David Planchard

April 24, 2015

Abstract:

The purpose of this MQP was to research, design, perform prototype iterations as well as develop a simple, reliable, light weight and cost effective ice fishing oscillating device for the recreational sportsman. In the sport of ice fishing, anglers operate numerous lines during the fishing process. Having a mechanism which utilizes the wind to oscillate the bait in the water makes the lure or bait more appealing to the fish. The device was created in an effort to improve fish yield. Several system iterations were created and tested until the final model served as an attachment for preexisting ice fishing tip ups. The model utilized the following components: turbine, oscillation mechanism, bushings, bi-pods, and base.

Executive Summary:

The purpose of this MQP was to research, design, perform prototype iterations and develop a simple, reliable, light weight cost effective ice fishing oscillation device for the recreational sportsman. In the sport of ice fishing, sportsman utilizes numerous lines during the fishing process. Having a mechanism which utilizes the wind to oscillate the bait in the water makes the lure or bait more appealing to the fish. The device was created in an effort to improve fish yield. Several system iterations were created and tested until the final model served as an attachment for preexisting ice fishing tip ups. The model utilized the following components: turbine, oscillation mechanism, bushings, bi-pods, and base. Research topics included; materials, mechanical properties, turbine designs, blade optimization, bearing functions, along with various kinematic and aerodynamic properties.

To date, three completely separate design iterations have been developed. After observing multiple malfunctions and design flaws in the preliminary designs, each new iteration was altered from the previous to both incorporate new design and manufacturing considerations, or address any optimization opportunities. The original focus of the design was to make an efficient, affordable, transportable fishing apparatus that was unlike any current product on the market.

In the first iteration, an anemometer inspired design was used, in which a vertical-axis wind turbine was used in conjunction with a 90 degree gear to transfer power to the shaft that ultimately jigged the anglers bait. The anglers bait is connected to a line that is winded onto a reel screwed into a device known as a tip-up. A tip-up consists of three thin pieces of wood that are arranged so that the tip-up is able to stand over a whole in the ice approximately 6-10 inches

in diameter. Like an X, Y, and Z axis, the center piece of wood stands vertically through the hole (Z-Axis), while the other two (X and Y Axis) form the base that the tip-up sits on. On the bottom of the vertical piece of wood, a reel is attached that lies underwater, where bait is connected to the associated line. On the top of the vertical piece of wood is a flag that snaps up if a fish bites the bait and takes line. As stated previously, the design ultimately became an attachment to this tip-up system. The anemometer cups were based upon researched couplets seen on many current turbine designs. A large goal was to use as much 3D printed material as possible in the design because of the low costs, strength, and versatility associated with PLA (Polylactic Acid) material. PLA is insoluble in water, lightweight, and less expensive than most 3D printing materials, which was an ideal material for the prototyping. Upon reviewing the original design it was found that the cost, friction, and complexity of a 90 degree transfer of power was ultimately inefficient for the production of the tip-up.

In the second iteration, further research was conducted and a horizontal-axis wind turbine was decided upon to remove with the 90 degree gear transfer. The new design entailed 4 weeks of research into the design of low wind speed turbine blades. Three separate airfoil profiles were found that would be proficient in low-wind speed scenarios, these blades would later be glued into their own separate center hub. All of the components were printed vertically out of PLA material in a 3D printer or from an alternative 3D printer using ABS (Acrylonitrile butadiene styrene) material. ABS is extremely similar to PLA but is more water resistant and has a higher melting point and extrusion temperature. The purpose of using ABS was because the school 3D printer uses ABS. To test the efficiency of each blade, simulated conditions with a box fan at various wind speeds was used. After the orientation and general design of the turbine was decided, the design of the base and construction of the system was investigated.

The first two iterations were developed as a singular all-in-one system, containing the turbine and tip-up all in one. This became a concern because of the size and maneuverability of the all-in-one system. One pressing concern was the marketability to anglers that already possess many tip-ups. For storage, transportation, and adaptability reasons it was decided to separate the tip-up from the turbine into two separate components for the third design iteration. The third design heavily addressed the transportation of the tip-up system. Originally the base was a stiff and rigid structure that was not foldable and contained far too much material.

This problem was solved when a system of foldable legs, held in place by pins in vertical and horizontal orientations was conceived. In this system each of the four legs of the base could be extracted from the Jig-Rite system and made the system easily transportable. When in place the system had the ability to be locked out in various conditions, which is vital when dealing with multi-variable conditions on the ice. An additional aspect considered was to raise the tip-up higher off of the ice. The addition included folded legs that are hinged to each of the current four legs. The angler simply needed to fold over the second half of the hinged leg and lock it into place with the latch. This addition was made so the angler could decide which height he or she would like the turbine to be at to catch various wind speeds.

After careful consideration and weeks of research, a second iteration of the bi-pod assembly was designed and constructed. The new design consisted of a spring locking system accompanied with a piece of PVC surrounding the leg. The spring acted on the PVC to push it into a locking notch on the steel base component. This system was suitable for testing and worked effectively for a three week period. Afterwards the wear from the constant testing and pressure from the springs bent the screws and ultimately made the base less stable.

For the fourth and final iteration a pin locking system was designed and chosen. The two-pin system eliminated multiple components from the third iteration as well as simplified the design for the user. A ball locking pin secured the each of the legs in either the standing or folded position. The angles of the brackets were also changed, after observing the need for more vertical support during testing.

Acknowledgements:

Table of Contents:

Table of Figures:

Nomenclature:

ρ_{air} **(kg/m³)**: Density of air

v_{min} **(mph)**: Minimum wind velocity

v_{max} **(mph)**: Maximum wind velocity

$r_{turbine}$ **(in)**: Radius of the turbine's swept area

d_{shaft} **(in)**: Diameter of the shaft

r_{cog} **(in)**: Radius of the cog that moves the slider

l_{shaft} **(in)**: Length of the shaft

ρ_{shaft} **(kg/m³)**: Density of the shaft

ρ_{cog} **(kg/m³)**: Density of the cog material

t_{cog} **(in)**: Thickness of the cog

ω **(rad/s)**: Rotational velocity

μ_k: Coefficient of friction between the slider and the guide

V_{slider} **(in³)**: Volume of the slider

θ **(°)**: Maximum angle between the link that connects the slider to the cog and the vertical

μ_b : Coefficient of friction of the bearings

C_d :Drag coefficient of the bait moving through the water assuming a cylindrical shape

A_{bait} **(in²)**: Approximated top area of the bait in the water

ρ_{water} **(kg/m³)**: Density of the water

μ_{as}: Coefficient of friction between the aluminum stopping ring and the steel bearings

n_{blade}: Number of blades on the turbine

α **(°)**: Angle of attack

C_L: Lift coefficient

l **(in)**: Chord length (for Reynolds number)

Re: Reynolds number

ν **(kg/(m*s)**: Kinematic viscosity

c (in): Optimal chord length

X_r: Tip speed ratio

B: Number of blades

r (in): Distance along blade length

Introduction:

A tip-up is a traditional ice fishing device that sits up on top of the ice but has spool with line that extends into a hole in the ice. Typically the angler uses an auger to drill a six to twelve inch hole in the ice in which the tip-up is placed into. The spool sits submerged in the water in the hole. Since the water pressure is greater than atmospheric pressure when ice is floating on a body of water, the water rises to nearly the top of the hole. This submerged spool keep the line from freezing so once the fish takes the bait/lure it can pull line off in free spool. There are many different styles of tip-ups that have arisen over the years, but the classic and most popular is the heritage tip-up.

The heritage tip-up has two cross members (x- and y-axis) and a vertical member (z-axis). The horizontal x- and y-axis members act as the foundation and keep the tip-up planted on top of the ice while centering the vertical z-axis member in the center of the hole. The line and bait can be set a desired depth below the surface. Once set, there is an alert mechanism in which a tab on the radius of the spool that extends inward. When a fish takes the bait, the spool spins, and that tab hits a lever which releases a flag that is sprung into the air. Thus, this action "alerts" the angler a fish has hit the bait. The bait usually used when ice fishing is live minnows. They do not sit stagnant in the water because obviously they are live minnows and swim around but do not trigger the alert.

There is another way of ice fishing called jigging. A shortened rod and reel is used in this case. The angler sits over the hole and physically oscillates or "jigs" the lure/ bait under the surface. This allows for different lures and baits to be used since the angler personally gives the lure or bait a vertical oscillating motion. Most types of fish are enticed by this lively action given

1

to the bait, so jigging for most species of fish, yields the best results. The angler is limited to jigging two rods, generally only one, because it requires one hand to reel and one hand to hold the rod. This is where there was an opportunity for improvement for the tip-up. The Jig-Rite system is able to harness the wind in order to oscillate multiple tip-ups, ensuring maximum fish yield for anglers.

Background:

History:

It is unknown when ice fishing truly began, but it is documented that Indian tribes have been doing the activity for hundreds of years. It was started by chipping away at the ice and using spears to stab fish as they attempted to attack a decoy (early forms of a fishing lure). As technique progressed in the early 1900s, a dowel with two golf tees attached to each end was used with a line attached dangling into the hole with a hook. Modern ice fishermen use what is now called a tip-up, or a small rod to catch their fish, which can be seen in Figure 1. Figure 1 is a standard ice fishing tip-up (Everything You Need for Fishing, n.d.). The cross base, seen in Figure 1 displays two horizontal arms which are centered over a hole when in use. The vertical piece of metal with the reel on the end of it is inserted into the hole so that the reel is under water to prevent the reel from freezing. When a fish hits the line creates a force that triggers a latch that in turn releases the flag, which signals a hit for the fisherman.

Figure 1: Standard Tip-up

Fishing started out as a means of hunting for food, progressed to a leisurely activity with the advancement of our food collection methods, and is now becoming a competitive sport in many areas. Fisherman are now looking for new ways to create an advantage against competitors and catch more fish. With advances in technology, ice fisherman began to develop ways to harness the wind to jig there baits for them, to potentially further entice a strike from a fish. To date there is only one product on the market that harnesses wind to jig the bait, which can be seen below in Figure 2 (Everything You Need for Fishing, n.d.).

Figure 2: Current Wind Powered Tip-up

This tip-up uses the wind to hit the wing (outlined in red circle) to move up and down and jig the bait a few inches. This type of jigging apparatus is not particularly effective. The jigging is not consistent, the bait only rises and falls a few centimeters, and the wing is only effective in a very small range of wind conditions.

Wind Turbines:

Since this device is to be powered by wind, some research into wind turbines was necessary. Wind power is one of the leading sources of renewable energy in the world right now, with more turbines being designed, manufactured, and put into the field daily. There are two

basic styles of wind turbines that are used today: horizontal-axis and vertical axis. Vertical-axis

turbines were used for initial iterations, since they do not have to be orientated in any particular

direction to function. A standard vertical-axis wind turbine can be seen in Figure 3 (Urban Green

Energy Vertical Axis Wind Turbine, n.d.).

Figure 3: Standard Vertical-Axis Wind Turbine

Horizontal-axis wind turbines were also investigated. The horizontal axis wind turbine is

the most efficient wind turbine available at this time. It operates at about a twenty percent higher

efficiency than a vertical axis wind turbine (Rogers, 2008). The only disadvantage for the

current application is a fixed horizontal axis turbine must be places relative to the wind direction.

The design for the horizontal axis is not only more efficient but it allowed for a direct transfer of

power and eliminated gears. The cog and slider component were responsible for oscillating the

bait and were directly attached to the shaft of the turbine, which is most ideal in terms of power transmission.

Materials:

Testing originally occurred with an acrylic and peak shaft, which were both donated to us by the IDEX Corporation. The idea behind testing with different shaft materials and diameters is to see if there is a noticeable change in efficiency. Different materials have more desirable mechanical properties, and different diameters require more energy to rotate, but will be more durable. In such harsh weather conditions, it is hard to hypothesize which material will perform best. PEEK (Polyether ether ketone) is a viable candidate because it is strong and stiff, which is a property needed to for a turbine shaft. PEEK is water resistant and its bearing grade has excellent wear characteristics. PEEK has a density of .047 g/cm^3 which makes it very lightweight. Acrylic is another viable candidate because it is very similar to PEEK. Like PEEK, Acrylic is also strong and stiff. It has a density of .044 g/cm^3 (Machinist Materials, n.d.). Acrylic is even more light weight as well as water resistant than PEEK but is less wear resistant than PEEK. Aluminum was another viable candidate for a shaft. Aluminum has a density of 2.7 g/cm^3 but being a metal, it is the most wear resistant and strong compared to the plastic alternatives (Aluminum 6061-T6; 6061-T651, n.d.). In the end the PEEK rod was the most efficient shaft for the turbine. The PEEK rod created the least amount of friction with the 3D printed bushings, was light weight, and also strong enough to deal with the environmental conditions.

The material used for the base of the turbine is a composite trim, specifically AZEK white PVC trim. It is light weight, durable, waterproof, and can be cut and worked just like wood, making it a suitable material for the base. As for the tip-up, a standard wooden tip-up was used to best replicate standard ice fishing scenarios.

6

The propeller is 3D printed and the material used is PLA. PLA is common in the extrusion process and after adjusting various extruder temperatures and speed settings, PLA yields a sufficiently smooth and accurate finish. This proved beneficial because no sanding or post extrusion machining was necessary. Since each propeller was comprised of three separate blades and a central hub after printing, LOCTITE Stick n' Seal Extreme Conditions was used to secure every component in place. PLA is not water resistant, so a waterproof coating was applied to the turbine once assembled to protect it from the harsh environment while ice fishing.

Goal Statement:

Design and manufacture an ice fishing consumer product that utilizes a wind turbine to oscillate an ice fishing bait vertically in the water to achieve a higher fish yield.

Design Specifications:

1. **Compatibility with tip-ups**: Universally compatible with 95%.
2. **Range of motion of the jig**: adjustable +/- .5 in (min) to +/- 3in (max).
3. **Weight**: less than 10lbs.
4. **Detachable**: Turbine separates from bi-pod base.
5. **Cost Goal**: Jig-Rite sells for approximately $60.00.
6. **Operating Temperature**: Functions in -30°- 80°F.
7. **Operating Wind Speed**: Operation capable in wind speeds of 5-30 mph.
8. **System Set Up**: 5 minutes (post hole drill).
9. **Water Resistant**: All components.
10. **Turbine Design**: Horizontal Axis.
11. **Assembly Break Down**: Breaks down in two minutes to fit into a 5 gallon bucket.
12. **Bipod Legs**: Legs are collapsible and have firm plant in ice.
13. **Line Oscillation**: Vertical within 3-4 degrees.
14. **Brake System**: Used to slow oscillation when desired.

Methods and Procedure:

Oscillation Mechanism:

One of the first steps was finding a way convert horizontally moving wind into a vertical oscillation of the bait. It was determined that the wind would be used to rotate a shaft, which would in-turn act on a kinematic device that would oscillate the bait. Three design iterations were created as a means of creating this oscillation.

Linkage System:

The first concept that was designed involved using a four-bar linkage to oscillate the bait. The linkage would meet Grashof conditions, so that the shaft could rotate in the same direction constantly, acting on the shortest link, thus creating a constant rotation of that link. The longest link would be fixed, so that the other link that was pinned to the longest link would move up and down as the shortest link rotated. A release clip holding the line would be attached to the opposite end of this link, so it would move the line, and ultimately the bait up and down in the water. There would also be six different holes at which the links could be pinned to change the range of oscillation from +/- 0.5 inches to +/- 3 inches, per specification. A SolidWorks model of this four-bar linkage can be seen in Figure 4.
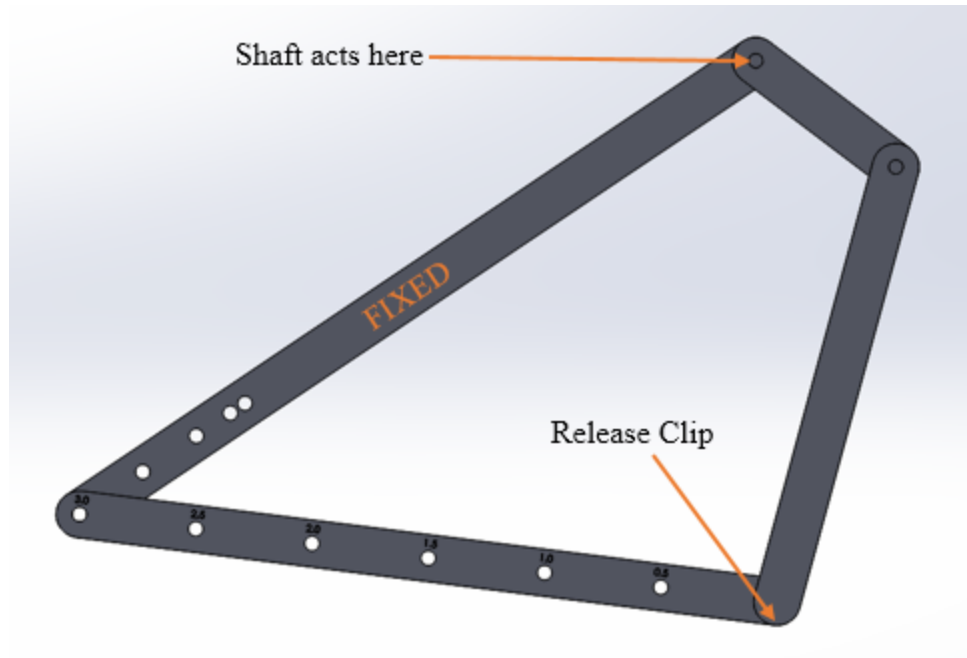
Figure 4: Four-Bar Linkage Oscillation Concept

Cam-Follower System:

The second concept that was designed for an oscillation system was that of a cam-follower system. The cam was designed as a perfect circle, with the shaft acting on a point at a distance of the desired jig range away from the center. The follower would have the release clip with the line attached, and would use a spring to create constant contact with the cam. As the cam rotated, the follower would be pushed downward, moving the bait downwards, and then pushed back upwards by the spring, pulling the bait upwards. A SolidWorks model of this concept (without the spring) is illustrated in Figure 5.

10
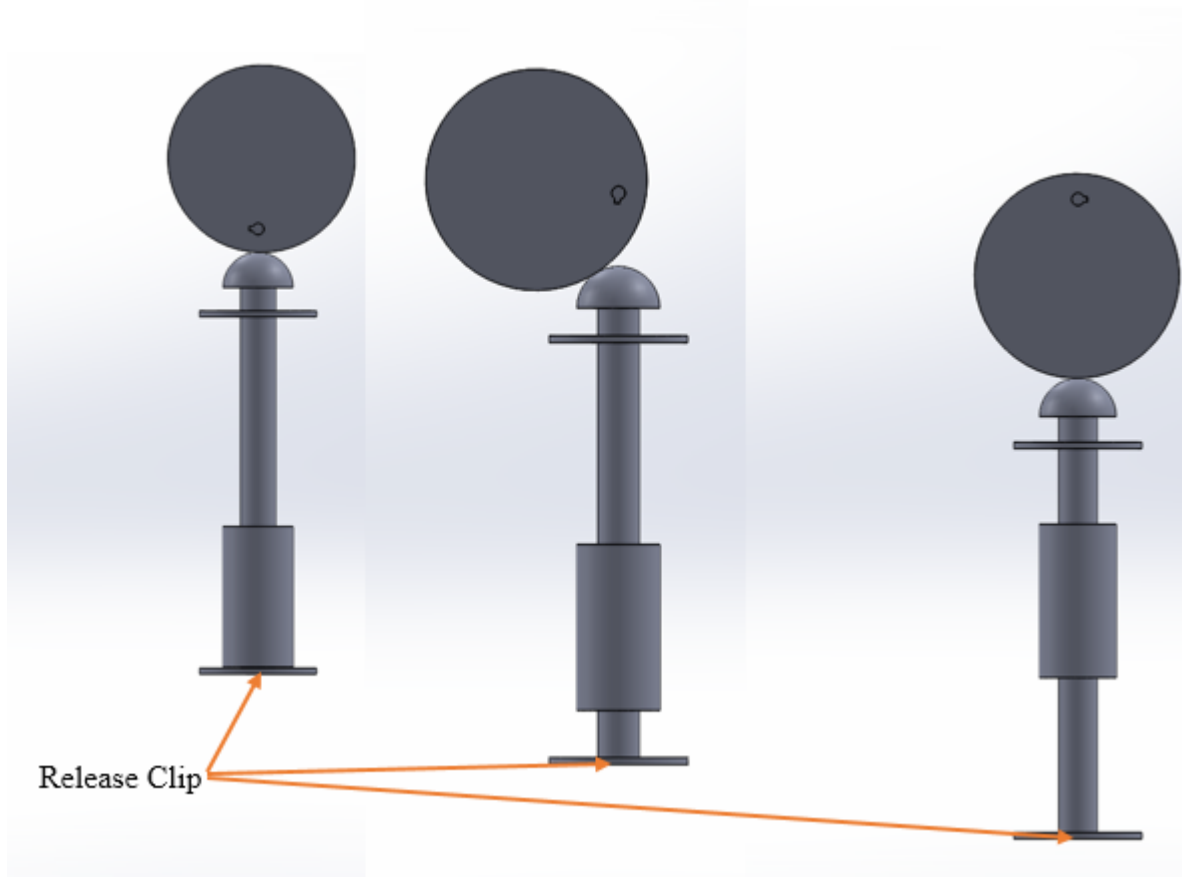
Figure 5: Cam-Follower Concept at Three Positions along Rotation

Cog-Slider System:

The third and final design used a cog and slider assembly to oscillate the bait in the water. The idea of the cog and slider was to keep the oscillation in a strictly vertical motion with as simple a component as possible. The cog is attached to the shaft of the turbine to achieve maximum efficiency in terms of power transfer. The cog and slider component in Figure 6 is a cog four inches in diameter. It has four pin holes which allows for a change is oscillation from half an inch to three inches. This is so the depth of oscillation can be changed based on fisherman preference.

A half inch oscillation will give the bait a twitch while a three inch oscillation will give the bait a more sweeping and diving motion. Depending on species of fish being targeted and lure or bait being used, this variation in depth is desirable.

The slider aspect of this component is to try to keep the bait moving mostly vertically which gives it the most realistic and natural look to the fish. The line will come up from the spool of the tip-up and attach to the slider. The slider is constrained loosely by a guide to keep the motion vertical. An arm is attached to the slider and a pin to the cog. The pin to the cog is the same pin mentioned previously to vary depths of oscillation. Some horizontal motion is expected because of drag due to lure and bait shape and the natural under water current. The slider is loosely constrained by the guide to eliminate any type of freezing that might occur. If the line is connected to the radius of the cog, the bait will have a less natural circular motion. The slider incorporates a release clip which will put enough tension and force on the line to hold it to the slider but will release upon the force of a fish taking the bait. Once released, the tip-up as a normal tip-up, free spool, and trip the flag alerting that a fish is running with the bait. The whole concept of allowing the line to un-attach from slider is that the fisherman, if necessary, can move the turbine out of the way and use the tip-up normally as if the turbine was never even there. This allows the fisherman to remove the tip-up from the hole and land the fish appropriately.
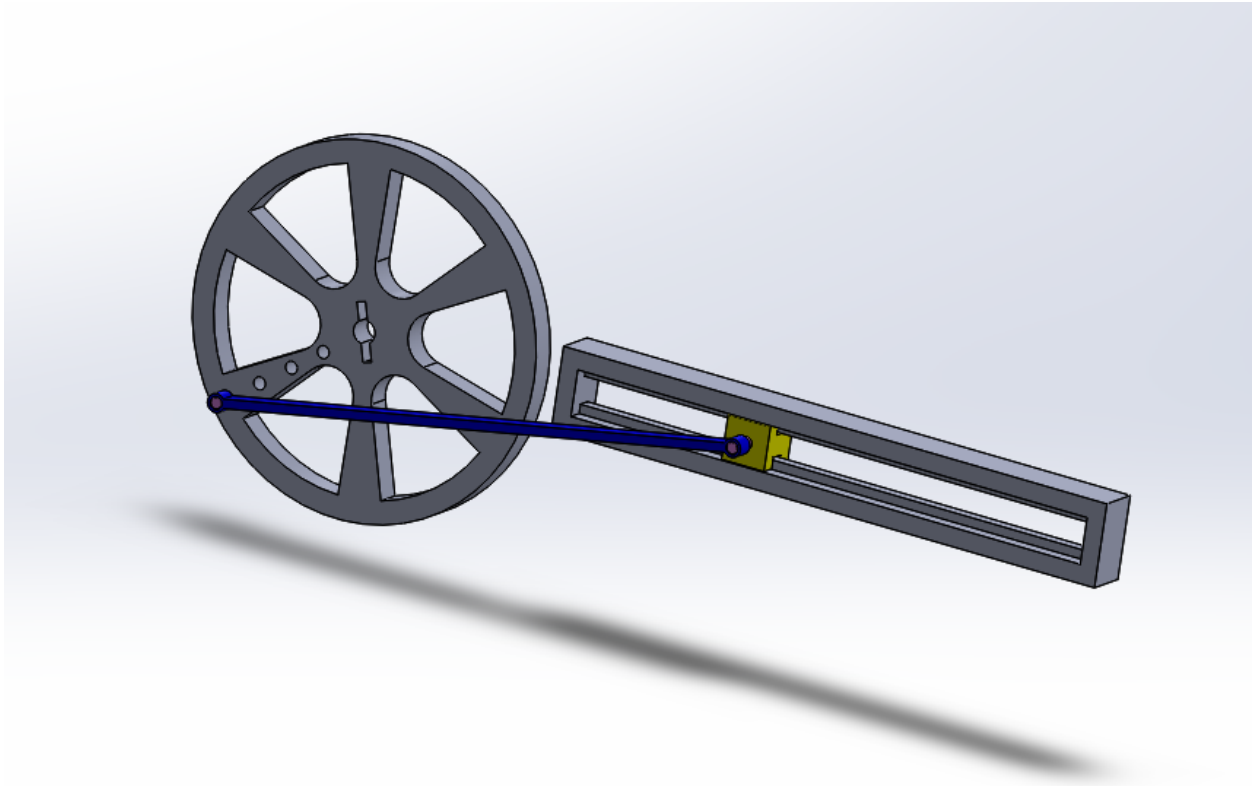
Figure 6: Cog-Slider Mechanism Concept

Final Decision

With three design iterations for an oscillation mechanism, it was then necessary to decide which one would be implemented into the final design. The linkage system was the first to be eliminated, since it is very large and bulky, not aesthetically pleasing, and the oscillation would not be perfectly straight up and down, but it would rather follow a slightly curved path.

The cam-follower system was the second to be eliminated. It would be more expensive to manufacture, as precise cams require high levels of precision which results in high manufacturing costs. When the cam was simulated in Dynacam, it resulted in a maximum pressure angle of 52.4°. The pressure angle is the angle between the perpendicular line between the cam and follower and the tangent line of the cam. Per specification, the pressure angle

13

needed to be below 30°, so this option was eliminated. The Dynacam simulation is illustrated below in Figure 7.

Figure 7: Dynacam Simulation of Cam Follower System

Ultimately, the cog system was chosen to be implemented in the final design. It is able to be adjustable to provide a jigging range of +/- 0.5 inches to +/- 3 inches, jigs the bait vertically in the water, and is very easy to add a damping mechanism to it. It is also very aesthetically pleasing and the simplest of the three concepts that were created and tested.

Turbine Type:

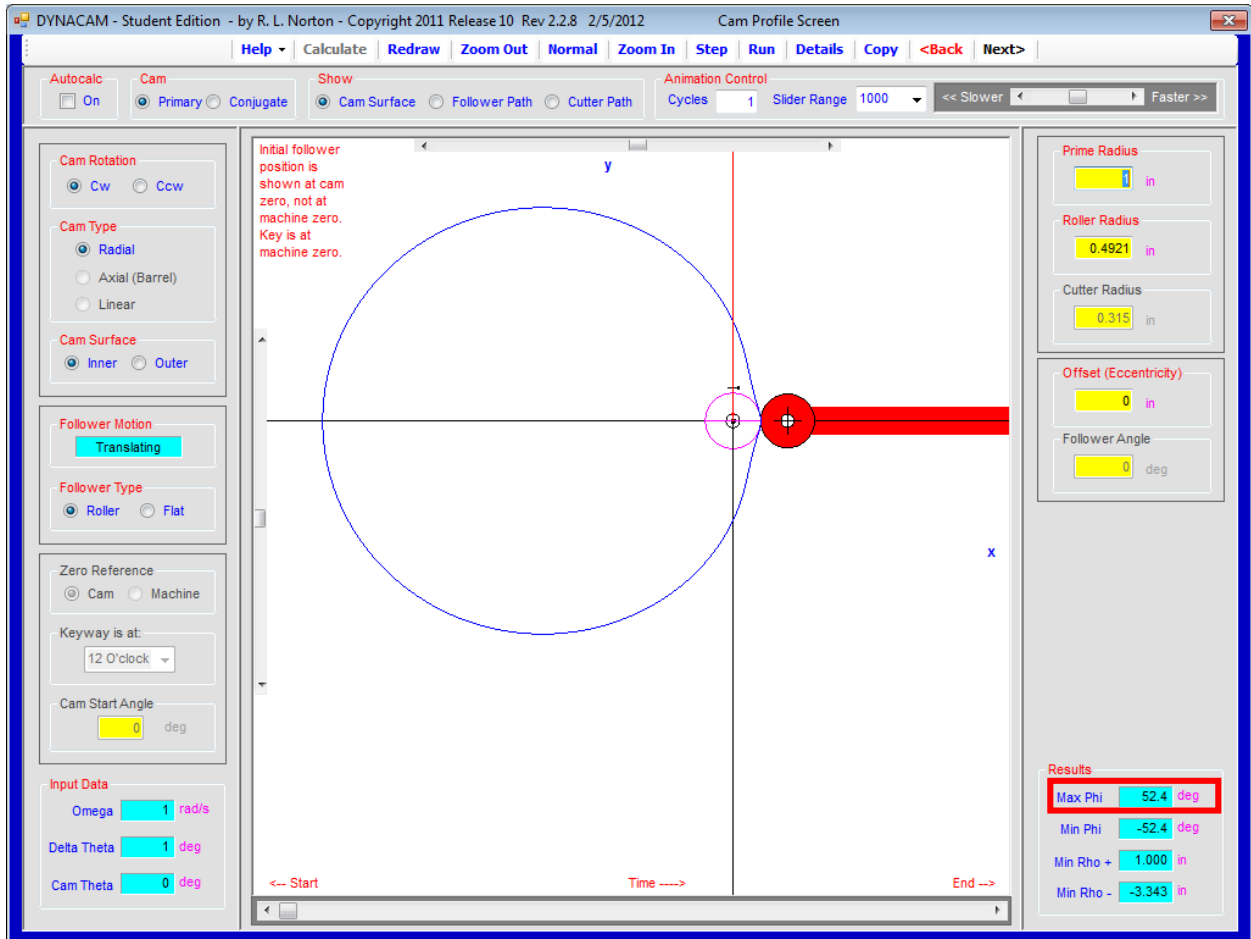An anemometer is a relatively simple way to harness and measure wind power. It is commonly a series of cups with different designs and dimensions. The advantage to a vertical axis turbine is that it will work independent of wind direction. As far as anemometer designs go, an elliptical face with a conical body was found to be the most efficient. It was also found that smaller cups with the same ratio of cup diameter to cups' center rotation radius result in higher rotational speeds (Pindado, Cubas, & and Sanz-Andres, 2013). The research performed was inconclusive in terms of the best dimensions to use for this small scale application. In the preliminary design, it was planned to experiment with different arm lengths, cup length to width ratios. Two design iterations were created for anemometer concepts. The first used elliptical cups with a rounded back and the second used circular cups with a conical back. These can be seen in Figure 8.
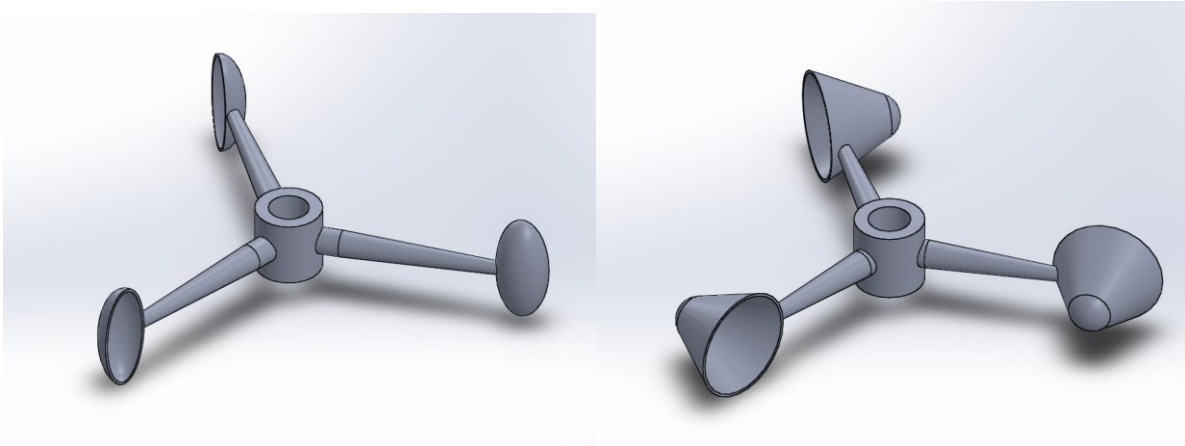

Figure 8: First Two Anemometer Design Concepts

The design incorporates a bearing in the bottom of the center of the anemometer to allow for rotation. The anemometer was to be placed on a vertical axis for rotation. The anemometer

15

would rotate a shaft and a 90 degree bevel gear would transfer power from the anemometer to a cog and slider responsible for oscillating the bait. Upon further research and designing, it was decided to retreat from this design for a number of reasons. First, anemometers are very inefficient compared to horizontal axis wind turbines. Second, bevel gears are difficult to print and work effectively and efficiently, and are costly to purchase. Plus given the icy conditions, the main concern was freezing and ice buildup which would render the gears useless. Horizontal axis wind turbines deemed to be a much more effective choice.

Base Design:

There were numerous iterations for the base and tip-up. The base needs to hold the turbine up high enough off the ice to be affected by wind because greater wind speeds occur higher off the ground. The spool would be submerged in the water to keep from freezing and allow free spool. The original design was to have the tip-up portion and the turbine be one structure. The base was going to accommodate a twelve inch in diameter hole in the ice, support the spool, alert system, turbine, and cog and slider. The turbine would sit three feet above the surface of the ice and would be eighteen inches wide. The spool would sit six inches underneath the surface of the ice so it would be submerged in the water. A SolidWorks model of this concept can be seen in Figure 9, and the constructed model can be seen in Figure 10.
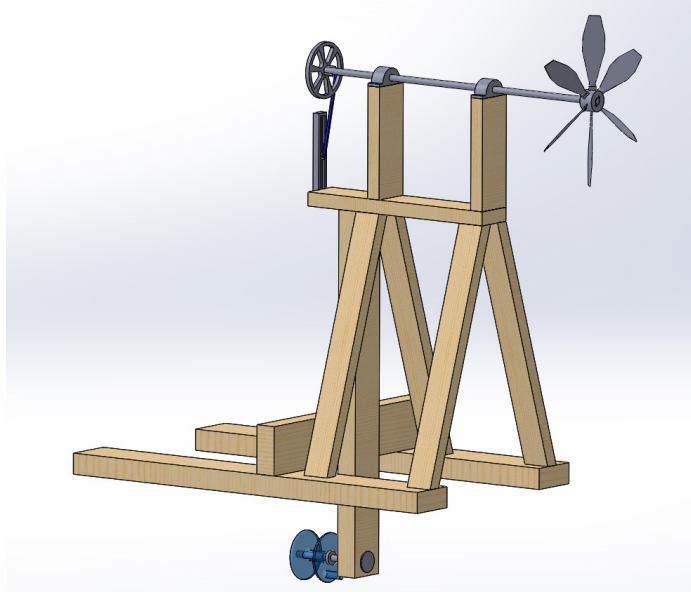
Figure 9: First Iteration of Base SolidWorks Model

Figure 10: Constructed Model of First Iteration of Base

After starting to build this design, it became apparent that there are many disadvantages

with this design. It is bulky and not easily collapsible or disassembled which makes it difficult to

handle and store. The next disadvantage is that once a fish is on the line, it is not easily removed from the hole. There was a design to add a hinged arm so it could be rocked back and hold itself up out of the hole so the fisherman could gain easier access to the line and hole, but that proper movement proved difficult to achieve. Ultimately this design shies away from the dexterity of a traditional tip-up.

The next iteration is a base completely separate from the tip-up. A single base like above with the turbine and other jigging components, all part of a single structure is detrimental to the tip-up aspect of ice fishing. The whole idea of a tip-up is to be a simple, easily set up mechanism that can be moved quickly out of the way once a fish strikes. To incorporate all the aspects that were originally planned into one tip-up just makes it bulky, difficult to assemble, and less portable. For this iteration, the turbine aspect is now a separate assembly from the tip-up. A tip-up that will be more compatible with this turbine than the traditional tip-up is also designed. The goal of this iteration is not to jeopardize the overall dexterity and ease of use of a standard tip-up and to enhance the productivity by giving the bait/jig/lure action. This design allows the tip-up to sit in the hole like a traditional tip-up, and the turbine will be separate and it will be placed over the hole alongside the tip-up. The assembly pictured in Figure 11 is just the turbine aspect. Bearings are added to the spindle, and the dimensions of the planks pictured are not final. It is just a representation of what materials were already available.

To make a base that is easier to transport and less complicated with various fixed pieces, there were a few different options considered. One option was a bipod or tripod design. The advantages would include; various heights for different wind speeds, retractable legs for storage, and a light and small design. Some of the disadvantages seen in this version were the costs of building or buying the legs, the ability for the material to last numerous amounts of cycles in the

18

cold wet temperatures, and the need to still be able to fold the legs upward for carrying them to the fishing hole. By using two of these for the base, the turbine system would be able to be mounted by four separate legs. A tripod design folds into one single vertical line but would not be the most practical for this base stand.

The next design incorporated a pin system, which allowed the legs of the base to move freely vertically and also horizontally when the pins are not in. When the pins are locked into position, the base's legs are restricted in vertical movement but not horizontal movement; thus allowing the fisherman to adjust for snow or ice conditions. Two separate chains will connect the front and back legs to keep the legs from slipping outward. One huge advantage to this system is the ability to separate the base and all of the legs from one another with the removal of the pins. Being able to store all components in a small bag or bucket could make the device much more appealing and much easier to carry. This concept can be seen in Figure 11. The assembly pictured below is just the turbine aspect. Bearings are added to the spindle, and the dimensions of the planks pictured are not final. It is just a representation of what materials are already available.

19
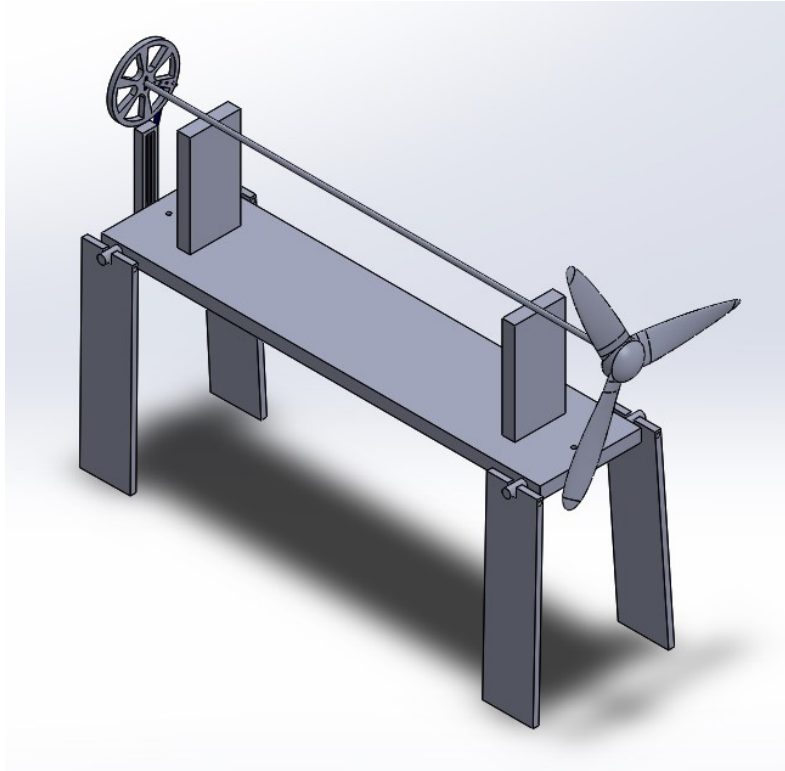
Figure 11: Second Iteration of Base SolidWorks Model

Bipods:

This base was determined to be unstable and too costly and difficult to manufacture. As a result, a pair of bipods was chosen to support the base which held the other components. Each bipod consisted of 2 legs that were secured to a metal plate that was bent at both ends. The legs were pinned in the center of the bent section of the plates and were allowed to rotate about that pin. The legs could be locked into the open position, in which they would extend at a 120° angle from the horizontal. They could be unlocked from this position to rotate so they would be horizontal with the base of the device. The advantage of this design was that, in the open position, the legs would provide a wide base to provide structural stability to the device and when closed, they would lie in line with the base, thus taking up less space and making the

20

device easier to transport. The SolidWorks model of the first iteration of the bipods can be seen in Figure 12.

Figure 12: SolidWorks Model of First Iteration of Bipod

The bipods consisted of the bent metal plate, 2 legs, and a locking mechanism. The original iteration for the locking mechanism was to JB Weld a metal ring and washer onto the legs that would support a spring. The spring would exert a force on a piece of PVC piping that had an inner diameter that was slightly larger than the outer diameter of the legs. The PVC would have a circular notch that could lock into a peg that would extend from the plate. When the legs were in the open position, the spring would push the PVC against the peg, locking the notch in the PVC into the peg on the plate. This concept was constructed and a picture of this concept can be seen in Figure 13.

21

Figure 13: Constructed Model of First Iteration of Bipod

The problem was that when the PVC was locked into place, there was nothing to prevent the PVC from twisting around the leg. This caused the legs to come unlocked from the open position and fold closed. This was unacceptable, as the legs needed to be able to resist any axial force exerted by the wind.

This led to a second concept to keep the legs locked in place. The spring-PVC system would be removed and rubber rings would be placed on each end of the leg. The wingnut on the end of the screw that pinned the leg to the plate could be tightened to cause the rubber rings to exert a friction force on the legs. This way, the legs could be moved to the open position and the wing nut would be tightened, effectively locking the legs in place. The same could be done for the closed position. The advantage of this system is that it didn't limit the number of positions at

22

which the legs could be locked, which could be useful if the device was being used on an uneven surface. This concept was constructed and can be seen in Figure 14.

Figure 14: Second Iteration of Bipod

This concept proved to be unusable as well, however. The friction force exerted by the rubber rings was not enough to keep the legs locked in any position, and the legs could be moved easily, even when the wingnut was tightened with great force.

The next concept for the locking mechanism reverted to the spring-PVC system, but this time, rather than using a circular notch and peg to keep the PVC in place, a metal slab would be secured to the plate and a long, skinny notch would be cut into the PVC. The theory was that this would make it harder for the PVC to twist because there would be no room for the notch to rotate. The circular shape of the first concept made it very easy to rotate, but the rectangular

shape of the new design would prevent this. This concept was constructed and photos of the bipod in the open position can be seen in Figure 15 and a photo of the bipod in the closed position can be seen in Figure 16.

Figure 15: Third Iteration of the Bipod in the Open Position

Figure 16: Third Iteration of the Bipod in the Closed Position

While this concept was an improvement on the first design, there was still some twisting that occurred. It also revealed a new problem that the legs, once locked into position, could be torqued away from the plate, thus unlocking the PVC from the locked position. Since the legs were cantilevered, and the long legs created a long moment, it didn't require much force to pull the legs out of the locked position. Also, having been used extensively, it was noticed that the screws that pinned the legs to the plate were starting to bend. This showed that larger screws had to be implemented to prevent bending.

The main problem with these bipods was that after a short time of use the hardware and PVC wore out quickly. The bipod legs did not lock into place easily or properly. The legs would fall out of place horizontally and the system would collapse. The final design that was used incorporated ball lock pins also known as hitch pins. ¼ - 20 bolts and wing nuts were used as the axis of rotation so the bipods can collapse and rotate to the standing position. Three total holes were placed in the bracket like the first iteration, one center hole for the axis of rotation, one hole for standing position, and one for collapsed position. The legs had two holes drilled 5/8" apart vertically down the leg for the hitch pins. The hitch pins are beneficial and superior because they exploit a small ball to lock the legs into position. The pins can easily and efficiently be removed and through the legs and bracket. The ball is responsible for applying pressure against the bracket to hold the legs in place. This does not allow for any movement in any direction and solves the problem of the legs collapsing horizontally outward. This bipod iteration is more user friendly and less complex and embraces design intent. A picture of this concept can be seen in Figure 17.

Figure 17: Final Bipod Design

Bushings and Bearings:

The original concept used bearings to house the shaft. Pillow block bearings from *CJ Bearings* were used. The bearings were actually adding more friction than relieving it as intended. Greasing the bearings made it even worse. A quick and effective solution was to use 3D printed bushings, which can be seen in Figure 18. The bushings worked very effectively. The only problem was preventing the turbine and shaft from sliding backwards from the force or the wind. To prevent the shaft from sliding, a nylon washer was fixed onto the shaft in front of the back bushing using a small set screw to keep the washer in place. The small area of plastic on plastic friction was negligible and did not affect the rotation of the turbine. The nylon washer can be seen in Figure 19 below.

Figure 18: 3D Printed Bushing

27

Figure 19: Nylon Washer with Locknut

Turbine Efficiency:

Once a horizontal axis wind turbine was decided upon, it was necessary to calculate the turbine efficiency necessary to make the shaft turn. Turbine efficiency is the ratio of the rotational energy of the shaft to the kinetic energy of the wind. To calculate this, the torque exerted on the system by the wind was first calculated at wind speeds of 5 mph and 15 mph, since the device needs to operate at a minimum wind speed of 5 mph, per specification. Initial variables were set up, with ρ_{air} equaling the density of air, v_{min} equaling the minimum wind velocity, v_{max} equaling the maximum wind velocity, $r_{turbine}$ equaling the radius of the turbine's

swept area, d_{shaft} equaling the diameter of the shaft, r_{cog} equaling the radius of the cog that moves the slider, l_{shaft} equaling the length of the shaft, ρ_{shaft} equaling the density of the aluminum the shaft is made of, ρ_{cog} equaling the density of the plastic the cog is made of, t_{cog} equaling the thickness of the cog, ω equaling the rotations per minute of the shaft, μ_k equaling the coefficient of friction between the slider and the guide, V_{slider} equaling volume of the slider, θ equaling the maximum angle between the link that connects the slider to the cog and the vertical, μ_b equaling the coefficient of friction of the bearings, C_d equaling the drag coefficient of the bait moving through the water assuming a cylindrical shape, A_{bait} equaling the approximated top area of the bait in the water, ρ_{water} equaling the density of the water, μ_{as} equaling the coefficient of friction between the aluminum stopping ring and the steel bearings, and n_{blade} equaling the number of blades on the turbine. The variables, moments of inertia of the shaft and cog, and torque exerted by the wind on the turbine can be seen in Figure 20.

$$\rho_{air} := 1.204 \, \frac{kg}{m^3} \qquad c_p := 0.59 \qquad v_{min} := 5mph \qquad v_{max} := 15mph \qquad r_{turbine} := 7.4in$$

$$d_{shaft} := 0.5in \qquad r_{cog} := 2in \qquad l_{shaft} := 24in \qquad \rho_{shaft} := 2.70 \cdot 10^{-3} \, \frac{kg}{cm^3}$$

$$\rho_{cog} := 1.21 \cdot 10^{-3} \, \frac{kg}{cm^3} \qquad t_{cog} := 0.3in \qquad \omega := 40rpm \qquad \mu_k := 0.1 \qquad V_{slider} := 0.09in^3$$

$$\theta := 16.95deg \qquad \mu_b := 0.0015 \qquad C_d := 1.2 \qquad A_{bait} := 1.5in^2 \qquad \rho_{water} := 1000 \, \frac{kg}{m^3}$$

$$\mu_{as} := 0.61 \qquad n_{blade} := 3$$

Moments of Inertia

$$m_{shaft} := \pi \cdot d_{shaft}^2 \cdot l_{shaft} \cdot \rho_{shaft} = 0.834 \, kg \qquad \text{mass of the shaft}$$

$$m_{cog} := \pi \cdot r_{cog}^2 \cdot t_{cog} \cdot \rho_{cog} = 0.075 \, kg \qquad \text{mass of the cog}$$

$$I_{shaft} := \frac{m_{shaft} \cdot d_{shaft}^2}{2} = 6.726 \times 10^{-5} \, m^2 \cdot kg \qquad \text{moment of inertia of the shaft}$$

$$I_{cog} := \frac{m_{cog} \cdot r_{cog}^2}{2} = 9.645 \times 10^{-5} \, m^2 \cdot kg \qquad \text{moment of inertia of the cog}$$

Torque on Turbine

$$P_{min} := 0.5 \cdot \rho_{air} \cdot \pi \cdot r_{turbine}^2 \cdot v_{min}^3 \cdot c_p = 0.44 \, W \qquad \text{Power generated under 5 mph wind}$$

$$P_{max} := 0.5 \cdot \rho_{air} \cdot \pi \cdot r_{turbine}^2 \cdot v_{max}^3 \cdot c_p = 11.886 \, W \qquad \text{Power generated under 15 mph wind}$$

$$T_{min} := \frac{P_{min}}{\omega} = 0.105 \cdot N \cdot m \qquad \text{Torque provided by 5 mph wind}$$

$$T_{max} := \frac{P_{max}}{\omega} = 2.838 \cdot N \cdot m \qquad \text{Torque provided by 15 mph wind}$$

Figure 20: Moments of Inertia of Cog and Shaft and Torque from Wind

Next, the area of the blade was approximated to calculate the wind pressure on the blade at 5 mph and 15 mph. These values were then used to calculate the thrust forces on the turbine, which would be used to calculate the force of friction on the stopping ring. These calculations can be seen in Figure 21.

$$A_{blade} := 6in \cdot 2in = 7.742 \times 10^{-3} \, m^2 \qquad \text{Surface area of one blade}$$

$$Q_{min} := \rho_{air} \cdot v_{min}^2 = 6.015 \, Pa \qquad \text{Wind pressure on blades for 5 mph wind}$$

$$Q_{max} := \rho_{air} \cdot v_{max}^2 = 54.138 \, Pa \qquad \text{Wind pressure on blades for 15 mph wind}$$

$$F_{thmin} := Q_{min} \cdot n_{blade} \cdot A_{blade} = 0.14 \, N \qquad \text{Thrust force on turbine for 5 mph wind}$$

$$F_{thmax} := Q_{max} \cdot n_{blade} \cdot A_{blade} = 1.257 \, N \qquad \text{Thrust force on turbine for 15 mph wind}$$

Figure 21: Thrust Force Calculations on Wind Turbine

The next step was to calculate the resistive torques on the shaft from the drag of the bait, the friction between the slider and guide, the friction of the bearings, the weight of the slider, and the friction between the stopping ring and the bearings. The torque caused by the bearings was calculated using an equation taken from ThyssenKrup Rothe Erde's website (Turning Torque Calculation, 2014). These calculations can be seen in Figure 22.

Drag Coefficient

$$F_D := 0.5 \cdot \rho_{water} \cdot (\omega \cdot r_{cog})^2 \cdot C_d \cdot A_{bait} = 0.026\,N \qquad \text{Force of drag on bait}$$

$$T_D := F_D \cdot r_{cog} \cdot \cos(\theta) = 1.278 \times 10^{-3} \cdot N \cdot m \qquad \text{Torque from drag on bait}$$

Torques

$$F_{gslider} := V_{slider} \cdot \rho_{cog} \cdot g = 0.018\,N \qquad\qquad \text{Weight of slider}$$

$$F_{fric} := \frac{\mu_k \cdot (F_{gslider} + F_D) \cdot \tan(\theta)}{1 - \mu_k \cdot \tan(\theta)} = 1.377 \times 10^{-3}\,N \qquad \text{Friction on slider}$$

$$F_N := (F_{gslider} + F_{fric} + F_D) \cdot \tan(\theta) = 0.014\,N \qquad \text{Normal force on slider}$$

$$F_{slider} := \sqrt{(F_{gslider} + F_{fric} + F_D)^2 + F_N^2} = 0.047\,N \qquad \text{Total force exerted by slider}$$

$$T_{slider} := F_{slider} \cdot r_{cog} = 2.399 \times 10^{-3} \cdot N \cdot m \qquad \text{Torque exerted by slider}$$

$$T_{bearing} := 2 \cdot \frac{\mu_b}{2} \cdot \left[F_{thmin} \cdot d_{shaft} + 2.2 \cdot (F_{slider} + m_{shaft} \cdot g) \cdot 2 \cdot d_{shaft} \cdot 1.73 \right] = 1.195 \times 10^{-3} \cdot N \cdot m$$
$$\text{Torque of bearings}$$

$$F_{fricringmin} := F_{thmin} \cdot \mu_{as} = 0.085\,N \qquad\qquad \text{Minimum friction on stopping ring}$$

$$T_{fricringmin} := F_{fricringmin} \cdot d_{shaft} = 1.082 \times 10^{-3}\,N \cdot m \qquad \text{Minimum torque on stopping ring}$$

$$F_{fricringmax} := F_{thmax} \cdot \mu_{as} = 0.767\,N \qquad\qquad \text{Maximum friction on stopping ring}$$

$$T_{fricringmax} := F_{fricringmax} \cdot d_{shaft} = 9.741 \times 10^{-3}\,N \cdot m \qquad \text{Maximum torque on stopping ring}$$

Figure 22: Calculations of Resistive Torques on Shaft

These torque calculations were then used to calculate the angular acceleration of the shaft at 5 mph and 15 mph. These calculations can be seen in Figure 23.

32

Acceleration

$$\alpha_{min} := \frac{T_{min} - T_{slider} - T_{bearing} - T_{fricringmin}}{I_{shaft} + I_{cog}} = 613.401 \cdot \frac{rad}{s^2} \quad \text{Angular acceleration at 5 mph}$$

$$\alpha_{max} := \frac{T_{max} - T_{slider} - T_{bearing} - T_{fricringmax}}{I_{shaft} + I_{cog}} = 1.725 \times 10^4 \cdot \frac{rad}{s^2} \quad \text{Angular acceleration at 15 mph}$$

Figure 23: Calculations of Minimum and Maximum Angular Accelerations of Shaft

Finally, these calculations were used to calculate the minimum possible turbine efficiency to make the shaft turn at a wind speed of 5 mph. These calculations can be seen in Figure 24.

Minimum Possible Efficiency

Given

$$T_{slider} + T_{bearing} + T_{fricringmin} = \frac{0.5 \cdot \rho_{air} \cdot \pi \cdot r_{turbine}^2 \cdot v_{min}^3 \cdot c_p}{\omega}$$

$$\text{Find}(c_p) = 0.026 \quad \text{Minimum efficiency to rotate shaft}$$

Figure 24: Calculation of Minimum Required Turbine Efficiency

This shows that the turbine requires a minimum efficiency of 2.6% to cause the shaft to rotate.

Turbine Design

Once it was determined that a horizontal axis wind turbine would be used, the next step was to design the turbine. Most of today's wind turbines use an airfoil shape as the cross-section

of each blade, so an airfoil was chosen to be used in the turbine blades for this project. There are many different profiles of airfoils, each serving a different purpose. An example airfoil profile, with the different parts named, can be seen in Figure 25 (How Airplanes Fly, n.d.).
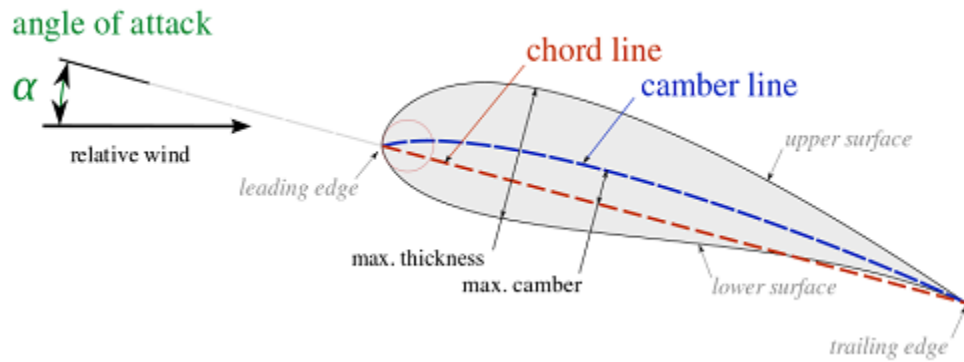

Figure 25: Airfoil Diagram

There are several naming systems for airfoil profiles, most commonly the NACA 4 digit system. Each profile is named with the letters NACA (National Advisory Committee for Aeronautics) followed by four numbers. In an airfoil named NACA-xxxx, the first digit represents the maximum camber of the airfoil in percentage of the chord length, the second digit represents the location of the maximum camber in tenths of the chord length, and the third and fourth digits represent the maximum thickness of the airfoil in percentage of the chord length (The NACA Airfoil Series, n.d.).

There are several preexisting airfoil profiles for which extensive research has been performed. Each profile has certain advantages and disadvantages. Profiles needed to be chosen for testing that would be best for the situations that the jigging mechanism will be encountering. Since the performance of airfoils is usually based around the Reynolds number experienced by the airfoil, this number needed to be calculated for the turbine being designed. Per specification,

this mechanism needed to function in wind speeds of at least 5 mph, so speed was used for the

calculations. Reynolds number is calculated with the equation $\text{Re} = \dfrac{vl}{v}$, where v is the wind

velocity, l is the chord length, and v is kinematic viscosity. Assuming a chord length of 1 inch, a

wind velocity of 5 mph, and a kinematic viscosity of 1341e-4 ft^2/s, which is the kinematic

viscosity of air at -10°C, a Reynolds number of 4,557 was calculated. Using this as a reference

point it was determined that an airfoil was needed that was suitable for ultra-low Reynolds

numbers (less than 10,000). This criteria led to the determination of three acceptable profiles;

NACA-0012, NREL-SG6042, and DAE-11.

These profiles were then used to create SolidWorks models of the first drafts of the

turbine blades. The first drafts of the NACA-0012 blade can be seen in Figure 26, the NREL-

SG6042 blade can be seen in Figure 27, and the DAE -11 blade can be seen in Figure 28.
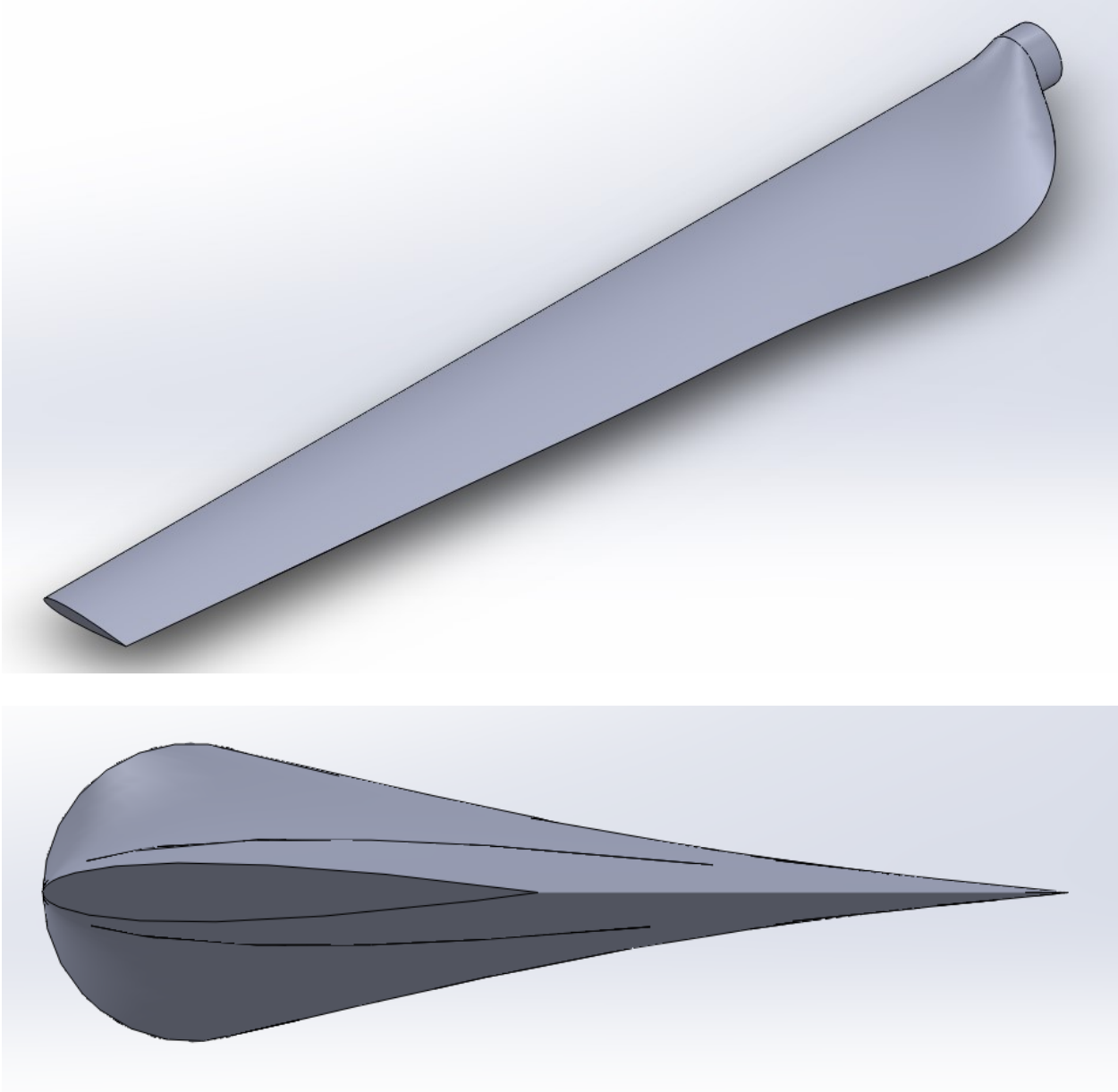
Figure 26: NACA-0012 Blade SolidWorks Model
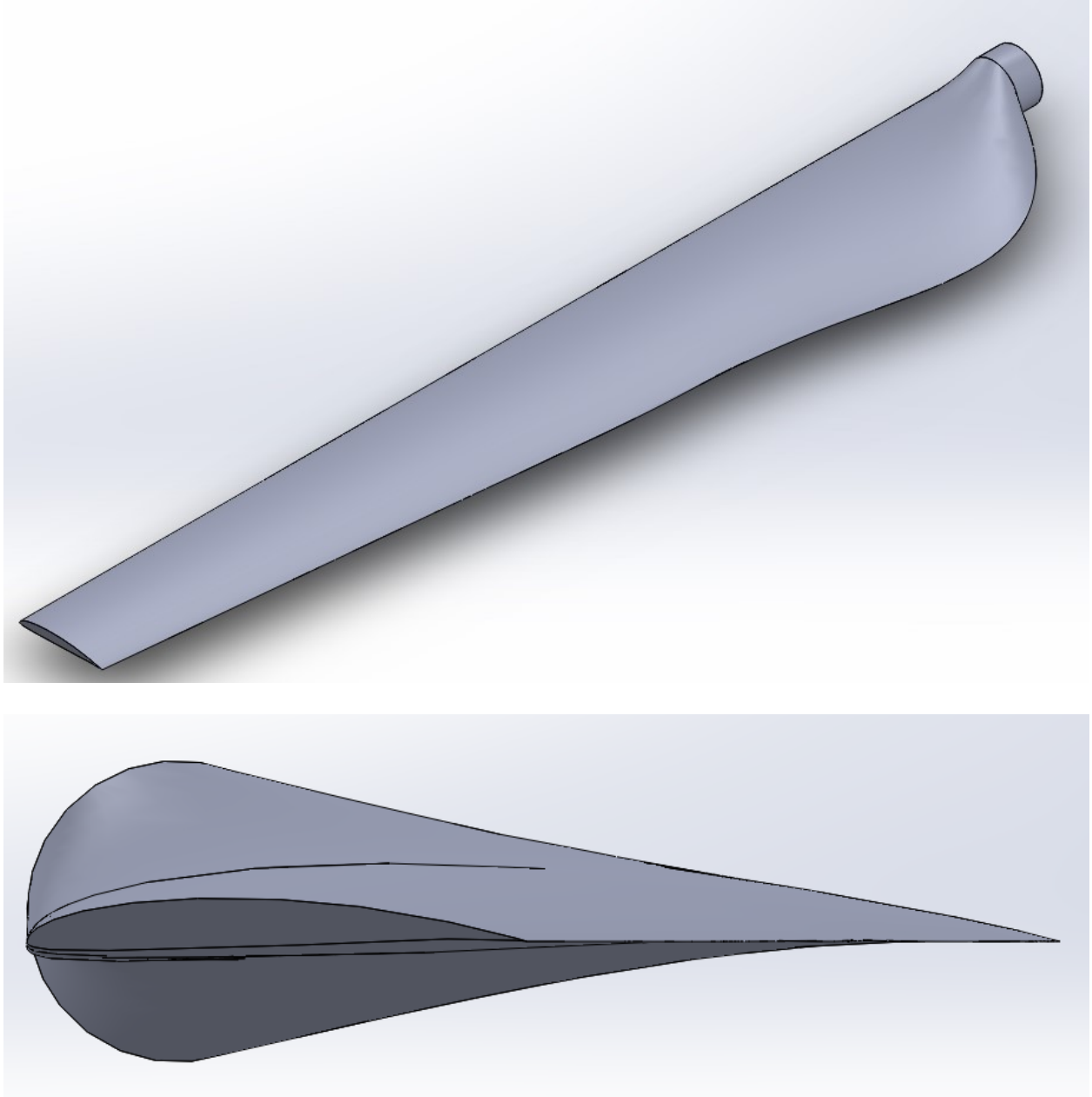
Figure 27: NREL-SG6042 Blade SolidWorks Model
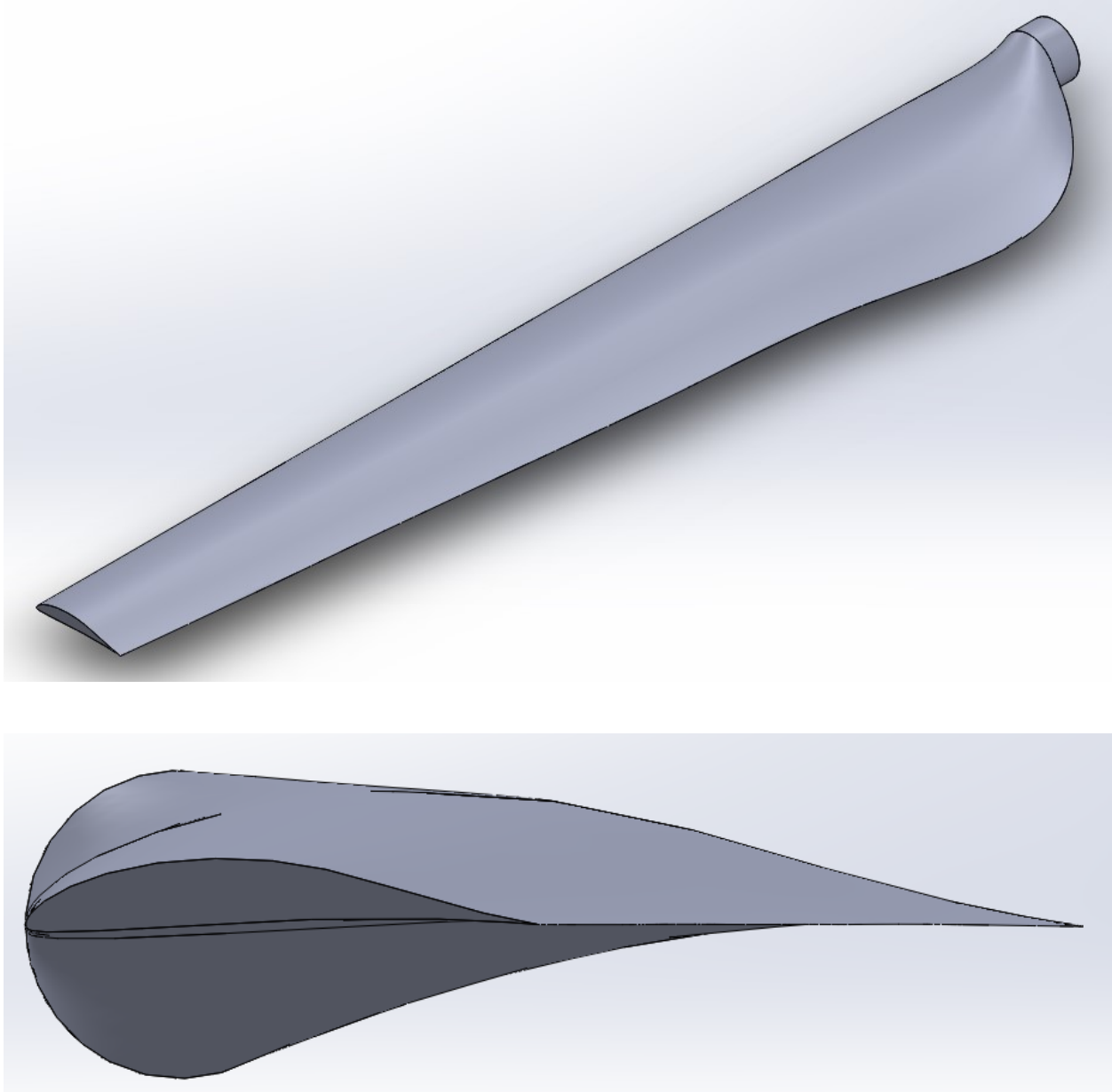
Figure 28: DAE-11 Blade SolidWorks Model

For each airfoil design, there is an ideal "angle of attack" that the blade should be inserted into the central hub at to achieve the highest lift coefficient. The lift coefficient is the amount of force the wind exerts to "lift" the blade, creating a rotation of the turbine. The angle of attack is the angle between the direction of wind and the chord line, as seen in Figure 25.

38

Previous testing has been performed on the different profiles to determine the angle of attack that

produces the maximum lift coefficient. A graph of angle of attack vs. C_L for the NACA-0012

airfoil can be seen in Figure 29 (Rumsey, 2014), for the NREL-SG6042 in Figure 30 (Lyon,

1997), and for the DAE-11 in Figure 31 (DAE 11 Characteristics, n.d.).
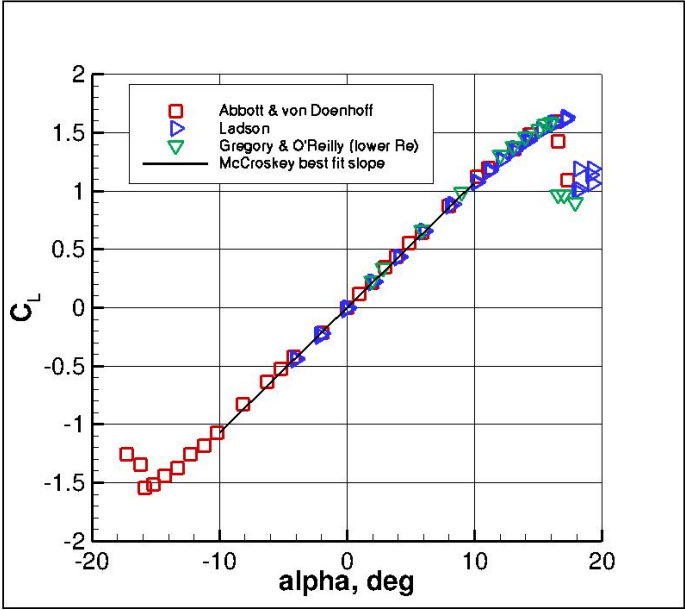
Figure 29: Angle of Attack vs. Lift Coefficient for NACA-0012 Airfoil
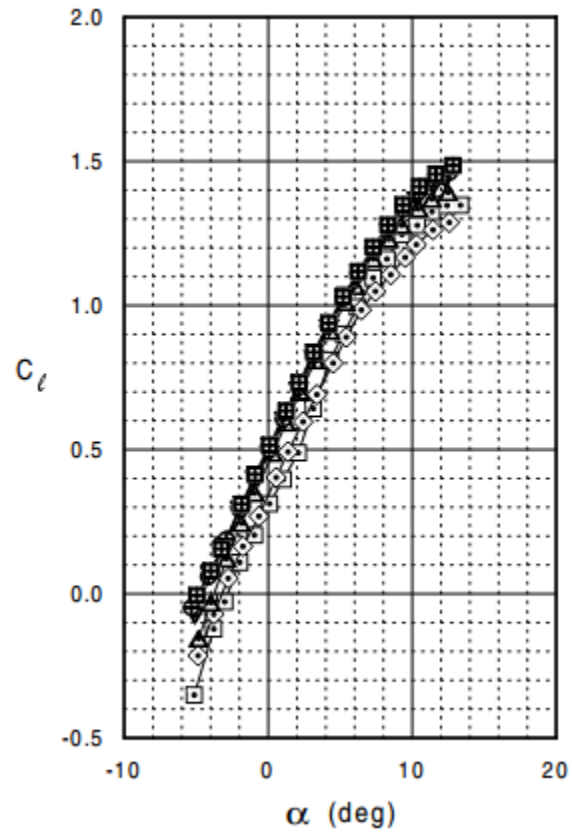
Figure 30: Angle of Attack vs. Lift Coefficient for NREL-SG6042 Airfoil
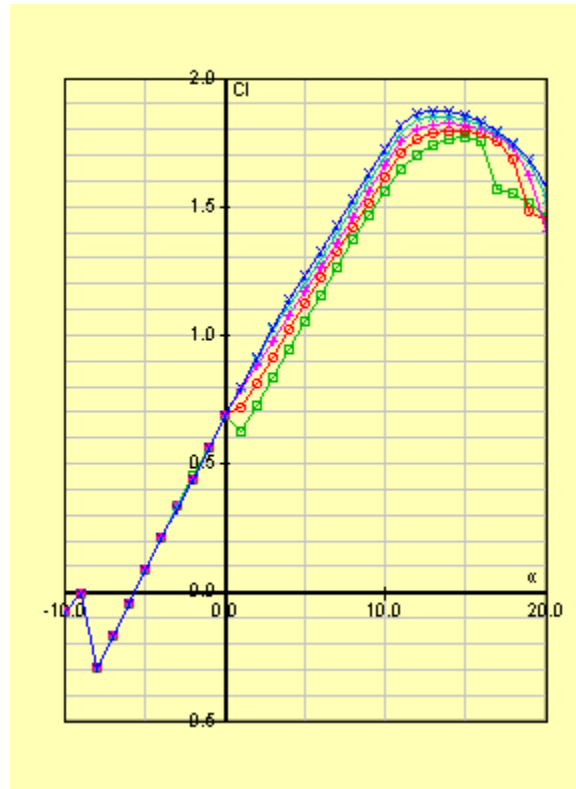
Figure 31: Angle of Attack vs. Lift Coefficient for DAE-11 Airfoil

This shows that the ideal angle of attack is about 17° for the NACA-0012, 11° for the NREL-SG6042, and 13° for the DAE-11.

At first, these blades were designed with the chord length decreasing by 0.1in/in across the length of the blade. When the first blade was 3D-printed, however, this produced blades that were far too thin to be structurally sound. This showed that the thickness of the blades needed to be increased so the blades would be stronger. The first iteration of the NACA-0012 blade printed with 15% infill can be seen in Figure 32, and with 40% infill can be seen in Figure 33.
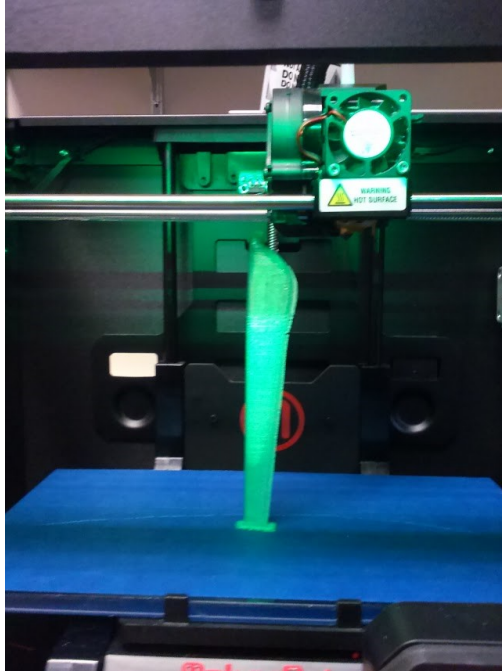
Figure 32: First Iteration of NACA-0012 Blade with 15% Infill
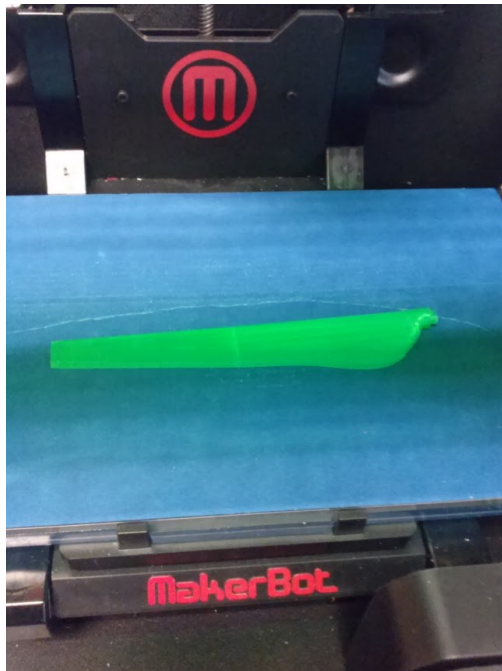
Figure 33: First Iteration of NACA-0012 Blade with 40% Infill

After the first iterations were made, the Schmitz equation was found, which relates the chord length with the distance across the turbine blade. This equation is

$$c(r) = \frac{1}{B} \frac{16\pi r}{C_L} sin^2 \left(\frac{1}{3} \arctan \left(\frac{R}{X_r} \right) \right)$$ (Gundtoft, 2009), where c(r) is the chord length at a

particular distance across the blade, B is the number of blades, r is the distance along the blade, C_L is the lift coefficient, R is the radius of the turbine's swept area, and X_r is the tip speed ratio which is the ratio of the speed of the tip of the blade to the wind speed. Tip Speed Ratio is calculated by $X_r = \frac{\omega R}{v}$, where ω is the rotational speed in rad/s, R is the radius of the swept area, and v is the velocity of the wind. This equation was used to calculate the chord length at six points across the length of the blade. The calculations of these chord lengths for the NACA-0012 blade can be seen in Figure 34. The distance along the blade and radius of the swept area takes into account the diameter of the central hub, which is 1.5 inches. The lift coefficient was taken from Figure 29, which shows a lift coefficient of 1.5 for the optimal angle of attack of 17°.

$$\omega := 40\text{rpm} \cdot 2\pi \qquad R := 7.4\text{in} \qquad v := 5\text{mph} \qquad B := 3 \quad C_l := 1.5$$

$$X_r := \frac{\omega \cdot R}{v} = 2.213$$

$$C_1 := \frac{1}{B} \cdot \frac{16 \cdot \pi \cdot 2.4\text{in}}{C_l} \cdot \left(\sin\left(\frac{1}{3} \, \text{atan}\left(\frac{R}{X_r \cdot 2.4\text{in}} \right) \right) \right)^2 = 2.59 \cdot \text{in}$$

$$C_2 := \frac{1}{B} \cdot \frac{16 \cdot \pi \cdot 3.4\text{in}}{C_l} \cdot \left(\sin\left(\frac{1}{3} \, \text{atan}\left(\frac{R}{X_r \cdot 3.4\text{in}} \right) \right) \right)^2 = 2.491 \cdot \text{in}$$

$$C_3 := \frac{1}{B} \cdot \frac{16 \cdot \pi \cdot 4.4\text{in}}{C_l} \cdot \left(\sin\left(\frac{1}{3} \, \text{atan}\left(\frac{R}{X_r \cdot 4.4\text{in}} \right) \right) \right)^2 = 2.27 \cdot \text{in}$$

$$C_4 := \frac{1}{B} \cdot \frac{16 \cdot \pi \cdot 5.4\text{in}}{C_l} \cdot \left(\sin\left(\frac{1}{3} \, \text{atan}\left(\frac{R}{X_r \cdot 5.4\text{in}} \right) \right) \right)^2 = 2.037 \cdot \text{in}$$

$$C_5 := \frac{1}{B} \cdot \frac{16 \cdot \pi \cdot 6.4\text{in}}{C_l} \cdot \left(\sin\left(\frac{1}{3} \, \text{atan}\left(\frac{R}{X_r \cdot 6.4\text{in}} \right) \right) \right)^2 = 1.825 \cdot \text{in}$$

$$C_6 := \frac{1}{B} \cdot \frac{16 \cdot \pi \cdot 7.4\text{in}}{C_l} \cdot \left(\sin\left(\frac{1}{3} \, \text{atan}\left(\frac{R}{X_r \cdot 7.4\text{in}} \right) \right) \right)^2 = 1.643 \cdot \text{in}$$

Figure 34: Calculations of Chord Length Across Blade Length for NACA-0012 Blade

These calculations increased the thickness of the blade, so they would in-turn be more structurally stable. A loft was created on SolidWorks to connect all six airfoil profiles and the circular part that would connect the blade to the central hub.

When the first iterations of the blades were being created, the angle of attack was thought to be the angle between the chordline of the airfoil and the direction of the actual wind that was blowing. It was later realized that the angle of attack was actually between the chordline of the airfoil and the *apparent wind*. The apparent wind takes into account not only the wind that is blowing, but also the relative wind caused by the rotation of the turbine. These two wind speeds can be combined with trigonometry to determine the apparent wind. A diagram of these wind speeds can be seen in Figure 35, where α represents the angle of attack.
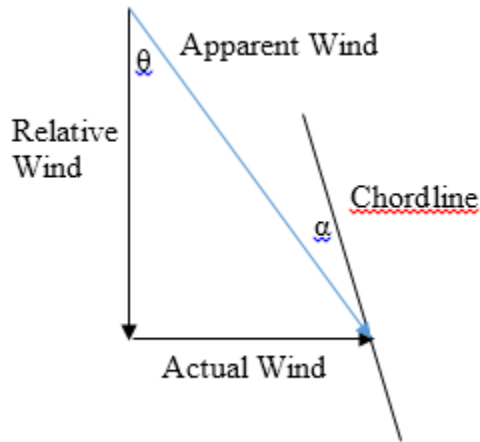
Figure 35: Diagram of Wind Speeds for Angle of Attack

Since the speed of each blade increases across the length of the blade, the angle between the blade and the direction of the wind needed to change across the length of the blade to create the ideal angle of attack. Since the relative wind increases linearly across the blade, a linear relationship was created between the distance across the blade and the angle between the relative wind and the apparent wind, which is represented by θ. The optimum angle of attack could then be subtracted from that angle to determine the angle at which the blade should be inserted into the hub. These calculations were first made for the NACA-0012 blade and can be seen in Figure 36.

$$\omega := 40 \text{rpm} \qquad v := 5\text{mph} = 2.235\,\frac{m}{s} \qquad \omega \cdot 2.4\text{in} = 0.255\,\frac{m}{s}$$

$$\theta_1 := \text{atan}\left(\frac{v}{\omega \cdot 2.4\text{in}}\right) = 83.483 \cdot \text{deg} \qquad\qquad \theta_1 - 17\text{deg} = 66.483 \cdot \text{deg}$$

$$\theta_2 := \text{atan}\left(\frac{v}{\omega \cdot 3.4\text{in}}\right) = 80.807 \cdot \text{deg} \qquad\qquad \theta_2 - 17\text{deg} = 63.807 \cdot \text{deg}$$

$$\theta_3 := \text{atan}\left(\frac{v}{\omega \cdot 4.4\text{in}}\right) = 78.171 \cdot \text{deg} \qquad\qquad \theta_3 - 17\text{deg} = 61.171 \cdot \text{deg}$$

$$\theta_4 := \text{atan}\left(\frac{v}{\omega \cdot 5.4\text{in}}\right) = 75.585 \cdot \text{deg} \qquad\qquad \theta_4 - 17\text{deg} = 58.585 \cdot \text{deg}$$

$$\theta_5 := \text{atan}\left(\frac{v}{\omega \cdot 6.4\text{in}}\right) = 73.057 \cdot \text{deg} \qquad\qquad \theta_5 - 17\text{deg} = 56.057 \cdot \text{deg}$$

$$\theta_6 := \text{atan}\left(\frac{v}{\omega \cdot 7.4\text{in}}\right) = 70.596 \cdot \text{deg} \qquad\qquad \theta_6 - 17\text{deg} = 53.596 \cdot \text{deg}$$

$$\theta_0 := \text{atan}\left(\frac{v}{\omega \cdot 1.5\text{in}}\right) = 85.916 \cdot \text{deg}$$

$$\theta_0 - \theta_6 = 15.32 \cdot \text{deg}$$

$$\theta_0 - 17\text{deg} = 68.916 \cdot \text{deg}$$

Figure 36: Blade Twist Calculations for NACA-0012 Blade

The difference between θ_0 and θ_6 of 15.32° is the twist from the base of the blade to the tip of the blade. A flex was applied to the SolidWorks model to incorporate this twist. The θ_0-17° angle of 68.916° was used to cut off a circular section of the base so it would fit to the hub and an extruded male part was added at that angle so the blade could be attached to the hub. The new SolidWorks model of this blade can be seen in Figure 37.
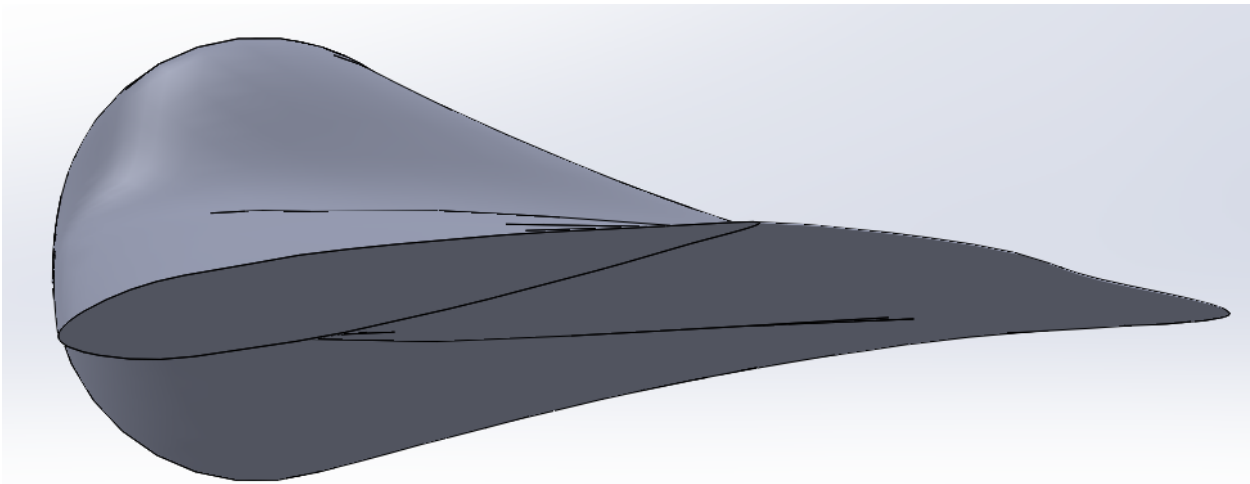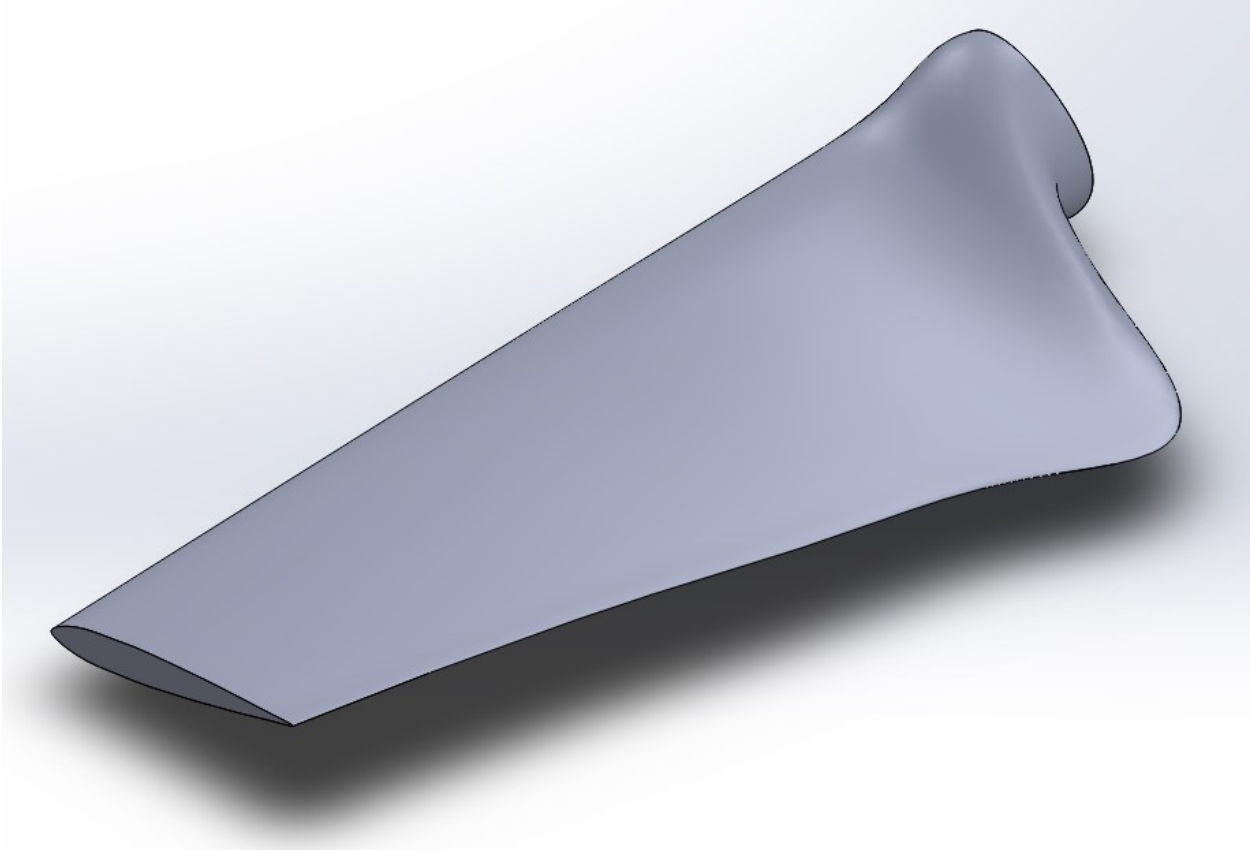
Figure 37: Second Iteration of NACA-0012 Blade SolidWorks Model

This SolidWorks model was sent to a 3D-printer to be printed. The resulting model can be seen in Figure 38.
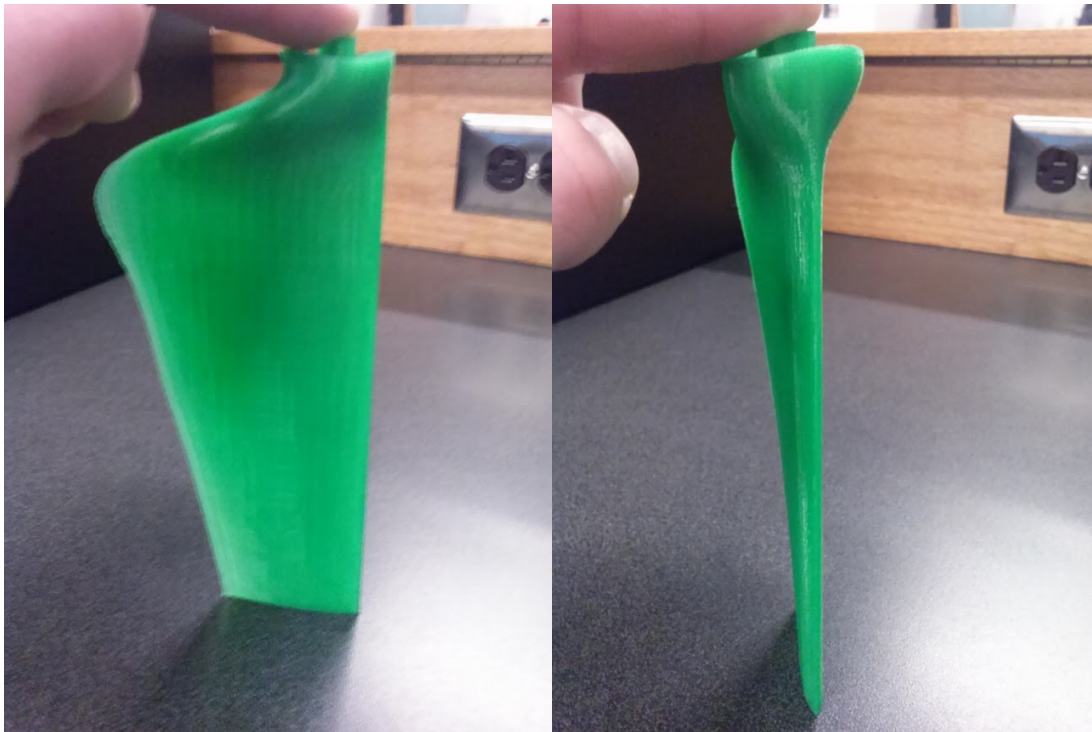
Figure 38: Second Iteration of NACA-0012 Blade

The central hub for the turbine was also printed. Due to cold temperatures during the printing process, the front and back of the hub were not printed correctly, and the back base of the hub was not properly attached. Ultimately, however, the main body of the hub was still functional enough to be used for testing. The hub contained a half inch hole in the middle (with a 0.01" tolerance) and the side of the hub had three equally spaced female parts for the blades to be attached (with 0.01" tolerances on the top and side). The central hub can be seen in Figure 39.
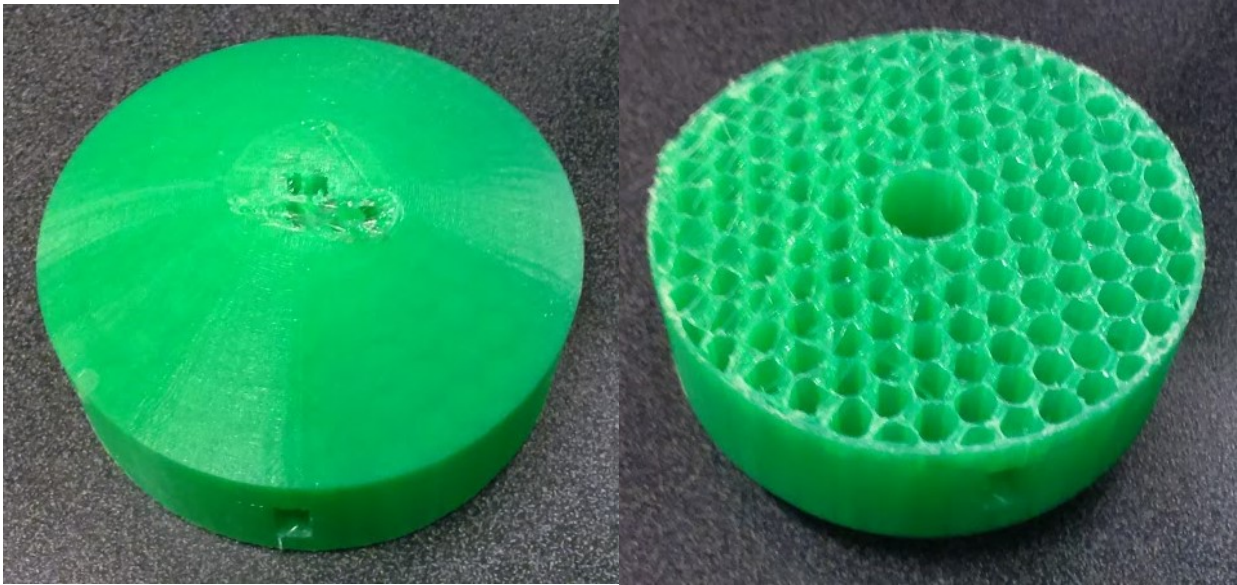
Figure 39: Turbine Central Hub

With all the parts for the NACA-0012 turbine printed, they were assembled by inserting the male ends of the blades into the female ends of the hub. The blades were secured to the hub using Loctite. The assembly can be seen in Figure 40.

Figure 40: NACA-0012 Turbine Assembly

The equation that related chordlength with the distance along the blade that was used for the NACA-0012 airfoil profile could be used for the NREL-SG6042 blade, since the length of the blades were the same. Calculations for the blade twist of the NREL-SG6042 blade were performed using the same method as with the NACA-0012 blade and can be seen in Figure 41.

$$\omega := 40 \text{rpm} \qquad v := 5 \text{mph} = 2.235 \frac{m}{s} \qquad \omega \cdot 2.4 \text{in} = 0.255 \frac{m}{s}$$

$$\theta_1 := \text{atan}\left(\frac{v}{\omega \cdot 2.4 \text{in}}\right) = 83.483 \cdot \text{deg} \qquad\qquad \theta_1 - 11 \text{deg} = 72.483 \cdot \text{deg}$$

$$\theta_2 := \text{atan}\left(\frac{v}{\omega \cdot 3.4 \text{in}}\right) = 80.807 \cdot \text{deg} \qquad\qquad \theta_2 - 11 \text{deg} = 69.807 \cdot \text{deg}$$

$$\theta_3 := \text{atan}\left(\frac{v}{\omega \cdot 4.4 \text{in}}\right) = 78.171 \cdot \text{deg} \qquad\qquad \theta_3 - 11 \text{deg} = 67.171 \cdot \text{deg}$$

$$\theta_4 := \text{atan}\left(\frac{v}{\omega \cdot 5.4 \text{in}}\right) = 75.585 \cdot \text{deg} \qquad\qquad \theta_4 - 11 \text{deg} = 64.585 \cdot \text{deg}$$

$$\theta_5 := \text{atan}\left(\frac{v}{\omega \cdot 6.4 \text{in}}\right) = 73.057 \cdot \text{deg} \qquad\qquad \theta_5 - 11 \text{deg} = 62.057 \cdot \text{deg}$$

$$\theta_6 := \text{atan}\left(\frac{v}{\omega \cdot 7.4 \text{in}}\right) = 70.596 \cdot \text{deg} \qquad\qquad \theta_6 - 11 \text{deg} = 59.596 \cdot \text{deg}$$

$$\theta_0 := \text{atan}\left(\frac{v}{\omega \cdot 1.5 \text{in}}\right) = 85.916 \cdot \text{deg}$$

$$\theta_0 - \theta_6 = 15.32 \cdot \text{deg}$$

$$\theta_0 - 11 \text{deg} = 74.916 \cdot \text{deg}$$

Figure 41: Blade Twist Calculations for NREL-SG6042 Blade

These calculations were used to create a SolidWorks model of the NREL-SG6042 blade. This model can be seen in Figure 42.
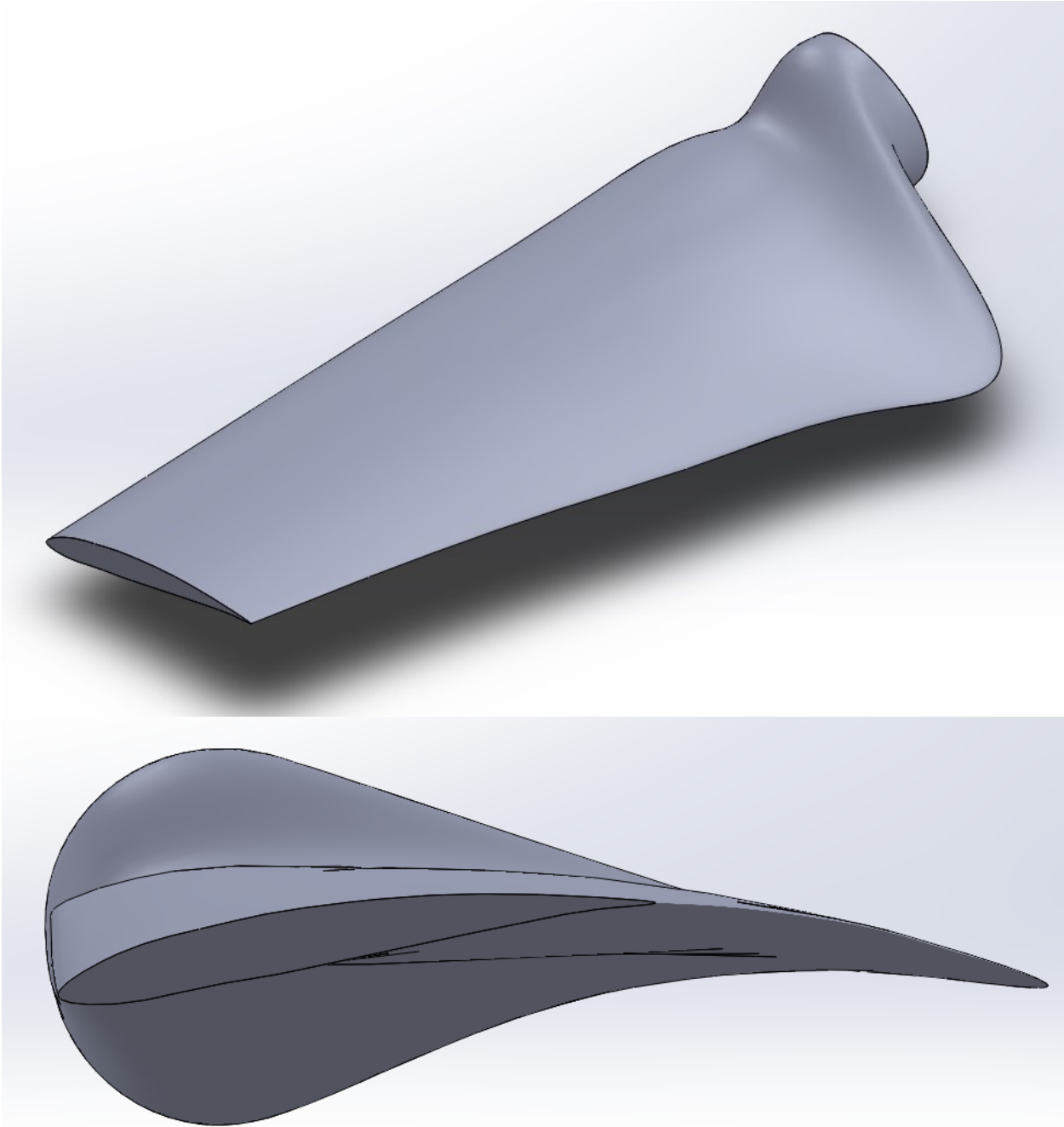
Figure 42: Second Iteration of NREL-SG6042 Turbine Blade SolidWorks Model

Three of these blades were 3D-printed with another central hub and were secured using Loctite. A picture of the final turbine can be seen in Figure 43.
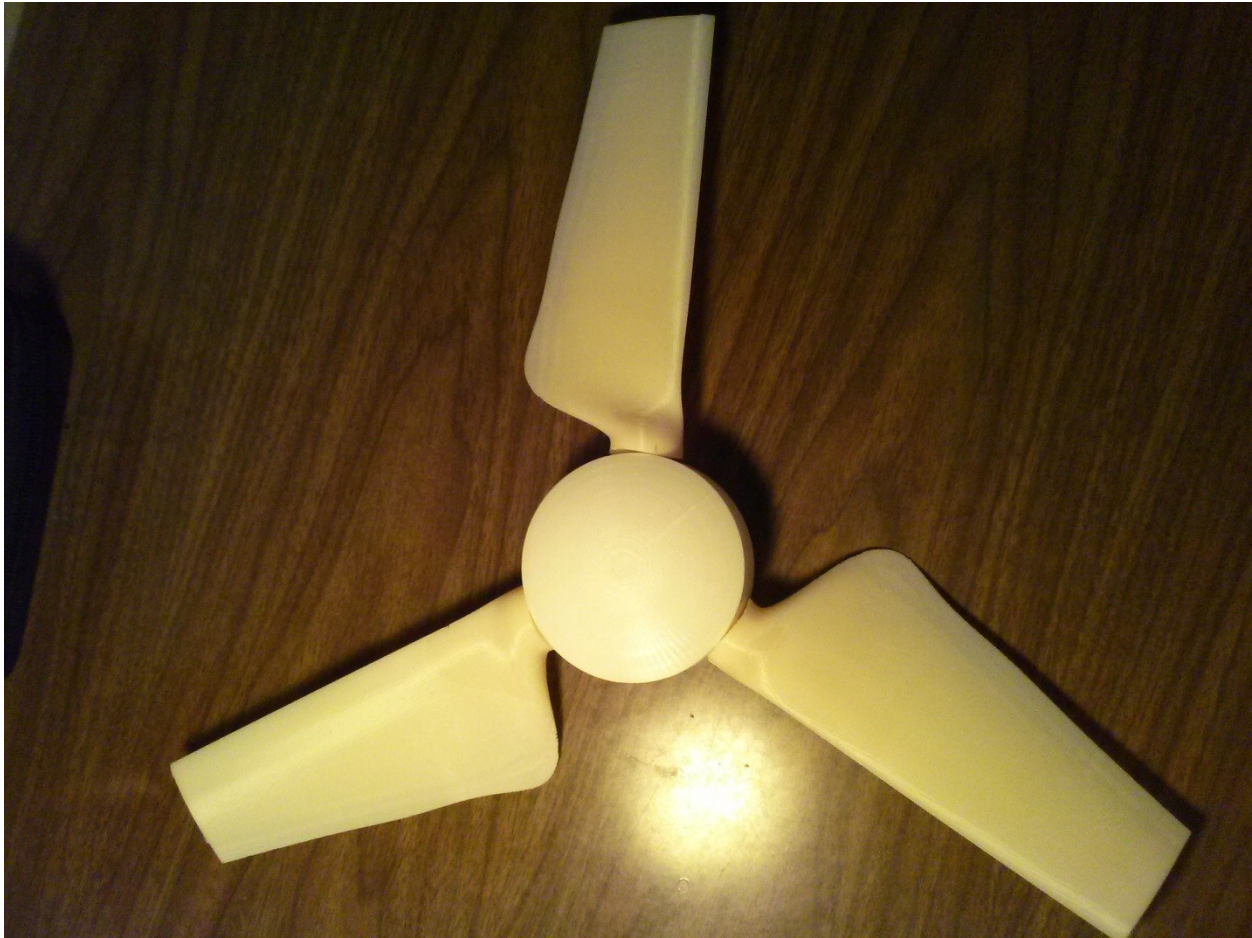
Figure 43: NREL-SG6042 Turbine Assembly

Due to time and budget constraints, it was decided not to 3D print a model of the DAE-11 turbine blade. Research on airfoil profiles showed that this profile would not be as effective at the anticipated Reynolds number the turbine would be experiencing as the NACA-0012 and NREL-SG6042 airfoil profiles.

Additive Manufacturing

For this project 3D printing was the most cost effective and efficient method for our prototyping process. Additive manufacturing refers to a technology where a work piece is created by adding layer upon layer of material to create a final product. 3D modeling software is

used to create a computer aided design model. An STL file is then loaded into a 3D printer to take the model from the software and print the 3D model.

After creating our two turbines in SolidWorks, a material had to be chosen to print them out of. Two of the most dominant plastics for 3D printing are Polylactic Acid (PLA) and Acrylonitrile butadiene styrene (ABS). PLA is more affordable but very susceptible to moisture and warping in an outdoor environment. ABS is water resistant but much more expensive. Two different turbine blades were printed one in each material to compare finish and ease of part mating. Both materials had a clean similar finish and mating the parts were fine as well.

ABS, PLA, and most other materials are porous when printed allowing moisture to seep into the part, so obviously an non water resistant material will not stand up to the harsh ice fishing environment. In attempt to waterproof the PLA, an epoxy and a water based polycrylic were experimented with. Those two water proofers were chosen because they were inexpensive and easy to apply and keep that smooth aerodynamic finish. Four PLA samples were coated. One with two coats of polycrylic another with four. And one with one coat of epoxy, and another with two coats because the epoxy went on much thicker. The first test was a chemical reaction test to see if either water proofer would react with the PLA. The polycrylic was water based and was expected to not have any reaction at all and was the safe decision in that sense, but was not expected to waterproof as well as the epoxy. After letting sit for three days, neither water proofer had a chemical reaction with the PLA. Next the samples were fully submerged in their own water container and checked twice a day at 8am and 8pm for three days. After the first twenty four hours the Polycrylic became white and pasty on the surface of the samples and it was evident the PLA was starting to break down. Both samples of epoxy remained clear and protected the PLA for the first 24 hours. After 36 hours it was found that the epoxy started to let

water degrade PLA samples as they were softer and more flexible. After three days all samples were much more malleable and degraded. It was determined one coat of epoxy would be sufficient to protect the turbine. It is recommended another coat be added after the first year of use or as seen fit. For future work, try looking into other 3D printing materials that are water resistant and inexpensive.

Benefits of additive manufacturing are that it allows for faster prototype work and experimentation. It cuts down manufacturing time because no tooling is necessary and there are less design limitations especially in terms of shape. Redesign and changes can be made quickly, and the parts are received much faster than traditional manufacturing. Multiple iterations can be made and even printed depending on part size in a matter of hours. The challenges that come with 3D printing are failed prints and determining print settings. There are many ways a print can fail. A change in temperature can cause the extruder to become clogged, the raw material can get caught in the spool and pull out of the extruder, and there might not be enough supports and the part might droop ruining design intent. Settings in the 3D printer software will usually have to be experimented with as well to get the result one is looking for in a final part. Percent infills affect part durability and how long prints take. Extruder speeds and temperatures affect surface finish. Part orientation is important because supports might have to be printed to hold the part up if the part has complex geometry. For example for the turbine blades, they were printed standing vertically so supports did not have to be broken off and ruin the integrity of the smooth aerodynamic face of the blade. Another problem is printer capabilities particularly size limitations. This turbine was printed so three separate blades mated with a separate central hub. The blades were 6 inches tall because the max height the printer was capable of printing was 6.1 inches.

54

Results:

Turbine Testing:

Once the two turbines were created, they needed to be tested in order to determine which one was more efficient. The first test that was performed was to measure the wind speed at which the turbines would start to turn. To do this, the device was set up in front of a standard room fan. The center of the turbine was aligned vertically and horizontally with the center of fan. The fan was put on its highest speed, and the device was moved closer to the fan until it was at the point where the blades just began to spin. At this point, a Kestrel 4000NV BT handheld anemometer was used to measure the wind speed at this location. The results of this test can be seen in Table 1.

Table 1: Turbine Startup Wind Speeds		
	Wind Speed at Blade Tip (mph)	Wind Speed at Turbine Center (mph)
NACA-0012	4.7	4.47
NREL-SG6042	6.93	6.49

This shows that the startup wind speed for the turbine with the NACA-0012 airfoil profile is lower than that of the turbine with the NREL-SG6042 airfoil profile. The wind speeds at both the blade tip and turbine center for the NACA-0012 turbine is lower than the design specification of 5 mph, while the wind speeds at both the blade tip and turbine center for the NREL-SG6042 were above the design specification. Ideally, this test would have been performed in a wind turbine, where the wind speed would theoretically be the same at the blade tip and turbine center, but this resource was not available. Ultimately, however, this test was sufficient enough to prove that the NACA-0012 turbine is more efficient than the NREL-SG6042 turbine and that the NACA-0012 turbine meets the design specification, while the NREL-SG6042 turbine does not.

55

The next test that was performed involved the same experimental setup as the first test, in which the device was set up in front of a room fan, but at a location in which both turbines would turn when exposed to the fan's wind. On each turbine, one blade was marked with a piece of duct tape so that it could be identified easier. The fan was turned on, and the turbine was allowed to rotate for 45 seconds, while being videotaped with a high-speed video camera. After this was done for both turbines, the video footage was analyzed to determine which had more revolutions in a 30 second period. Each turbine was given 5 seconds to start rotating and build up some rotational speed, then the number of times that the marked blade passed the top of the rotation in 30 seconds was counted. The video was slowed down to 1/32 speed to accurately count the number of rotations. An anemometer was used to measure the wind speed at the blade tips to be 6.93 mph and 6.71 at the turbine center. The number of rotations in 30 seconds was multiplied by 2 to get the average number of revolutions per minute (RPM's). The results can be seen in Table 2.

Table 2: Revolutions Per Minute at Operating Speed	
	Revolutions Per Minute
NACA-0012	285
NREL-SG6042	120

Ice Testing:

When the device was used on the ice, it was able to capture 3 fish in a 2 hour span, compared to a traditional tip up that caught only 1 fish. Further testing is necessary to fully gage the capabilities of the device compared to a normal tip up.

56

Troubleshooting:

When construction of the first prototype of the device was completed, it was taken onto the ice to determine how it would function under normal ice-fishing conditions. When exposed to wind, the turbine rotated, just as it was expected to, turning the cog which in turn raised and lowered the line holding the release clip. The release clip held the fishing line with the jig in the water, and an underwater camera was able to record the motion of the underwater jig. After examining the footage and by watching the device function above water, several problems were noticed that needed to be corrected.

The most evident problem that needed to be resolved was that there needed to be a guide for the line holding the release clip. When the wind speeds were low, the oscillation motion was primarily vertical, but still had some side to side motion. At higher wind speeds, the line was being pulled violently in a circular motion, causing a lot of side to side motion of the jig. To solve this, a screw with an eye hole bent at 90° was added to the bottom of the base. The line holding the release clip was fed through this then attached to the cog. When the shaft turned, the guide transferred the circular motion of the cog into strictly vertical motion of the release clip and jig in the water. This also prevented the line from wrapping around the shaft when it was pulled with very high wind speeds. A picture of this guide can be seen in Figure 44.

Figure 44: Line Guide

Another issue that was immediately noticed was that high wind speeds caused the turbine

to rotate too fast to the point where the line was being jigged out of control. As the turbine

turned, the line would be jigged upwards as desired, but the high rotational velocity didn't give

the jig enough time to sink back down before being jigged up again. The underwater video

footage showed the jig oscillating as expected while the turbine was turning slowly, but when it gained velocity, the jig remained at the top of the oscillation range and was getting whipped side to side. These high velocity winds also caused the line to be pulled so hard that it would whip upwards and wrap around the shaft. To solve this problem, a brake was added to the device. A rectangular piece of aluminum was attained, a hole was drilled through the front face, and two holes were drilled through the top. The hole on the front face was tapped for a ¼-20 screw. The two top holes were used to fasten the block to the base of the device. A ¼-20 thumb screw was fed through the hole on the face of the block, towards the shaft of the device. A rubber expansion nut was screwed on the end of the thumb screw with Teflon tape to hold it in place. This would allow the angler to tighten the thumb screw so that the expansion nut would make contact with the shaft, adding frictional resistance. As the wind speed increased, the angler could tighten the screw more, thus increasing the resistance. This brake was inserted close to one of the bushings to decrease the bending of the shaft. A picture of this brake can be seen in Figure 45.
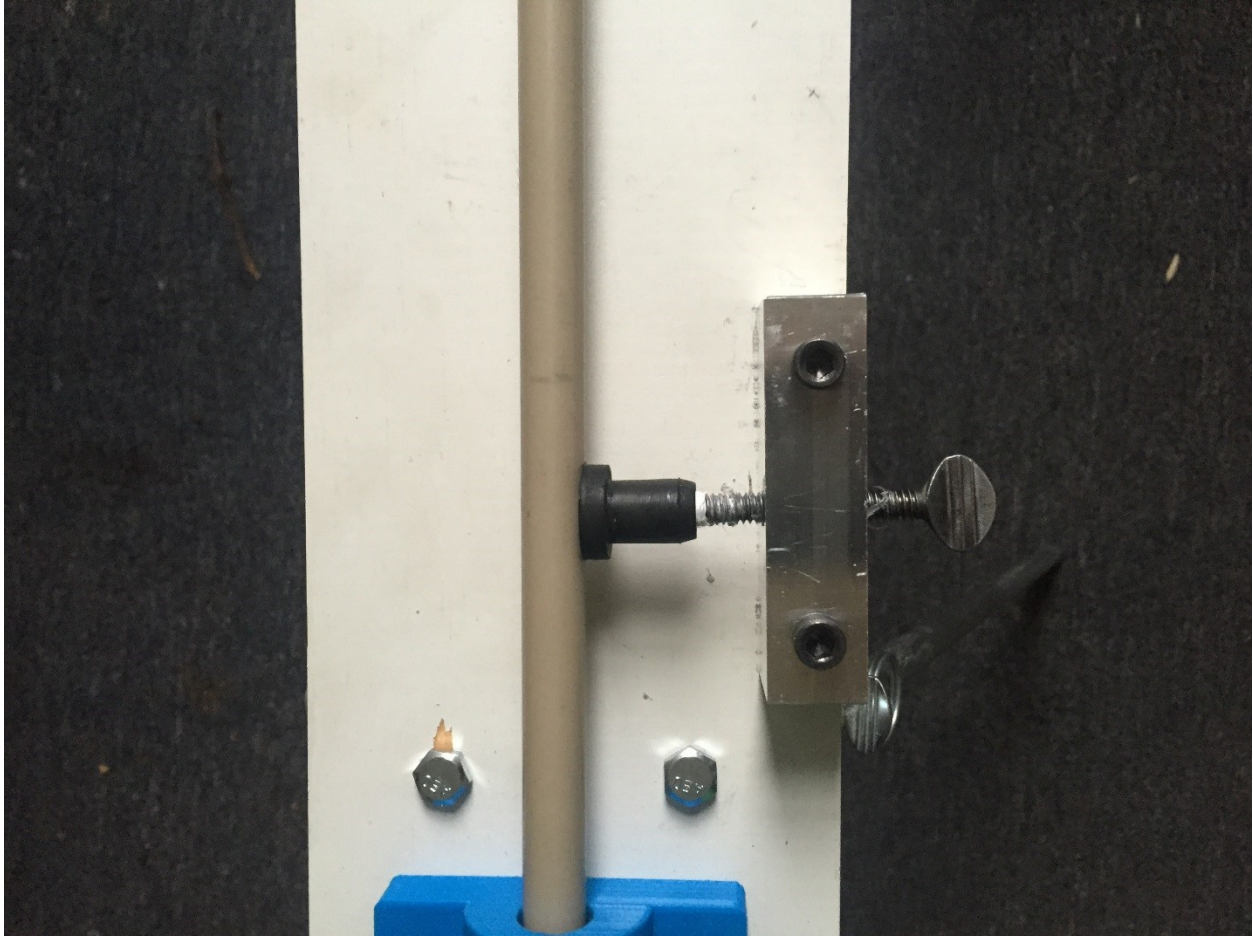
Figure 45: Brake Applied to Shaft

Another problem that occasionally happened at the beginning of the testing was that when the line was pulled from the release clip, it would fall on top of the reel that was submerged in the water. The solution to this did not require a change to be made to the device, but rather simply moving the tip up to the opposite end of the fishing hole of the device. The angler must make sure this is done when using this device. Also, the testing was being done with a 6 inch diameter hole, which is the size of the smallest auger that is commercially available. Most holes are 8 inches or larger, so this extra space would further ensure that the line does not land on top of the reel.

Recommendations:

Recommendations for later work and areas of improvement are:

1. Investigate the use of solar power as an alternate source of energy when there is a lack of wind.
2. Include a feature so turbine direction matches changing wind direction.
3. Create more effective release clip.
4. Reduce cost of the system to $50.
5. Make bipods more manufacturable.
6. Have interchangeable parts for different occasions.
7. Different bushings that dampen rotation.
8. Work with larger or smaller cogs.
9. Larger Cog with holes spaced.
10. Investigate alternative turbine and shaft materials.
11. Explore injection molding technology for turbine blades.
12. Additional testing in conditions where ice build-up is more prevalent.

Conclusion:

The purpose of this MQP was to design and manufacture an ice fishing consumer product that utilizes a wind turbine to oscillate an ice fishing bait vertically in the water to achieve a higher fish yield. Two wind turbines were designed, 3D-printed, and tested, with the turbine with the NACA-0012 airfoil profile being better than the one with the NREL-SG6042 airfoil profile. Multiple concepts were designed for an oscillation device, with a cog and guide ultimately being implemented. The device was originally meant to include the rod and line, but it was changed so that it could be used as an attachment to 95% of commonly used tip ups. This led to many iterations of bipods to hold the base off of the ice, with the final design implementing two bent plates that held aluminum legs that locked into an open or closed position using a hitch pin. During testing, it was found that fast wind would make the turbine rotate too quickly, causing the line to become tangled and not function as intended. To counteract this, a brake was added to

slow it down when necessary. When implemented on the ice, it functioned as intended, and was

able to catch 3 fish in a two hour testing period.

References

Aluminum 6061-T6; 6061-T651. (n.d.). Retrieved from ASM Aesospace Specification Metals

    Inc.: http://asm.matweb.com/search/SpecificMaterial.asp?bassnum=MA6061t6

DAE 11 Characteristics. (n.d.). Retrieved from Prop Designer:

    http://library.propdesigner.co.uk/html/dae_11_characteristics.html

Everything You Need for Fishing. (n.d.). Retrieved from 4fishin.com:

    http://www.4fishin.com/ht_tipups.htm

Gundtoft, S. (2009, June). *Wind Turbines*. Retrieved from University College of Aarhus:

    http://staff.iha.dk/sgt/Downloads/Turbines%20May4_2009_1.pdf

How Airplanes Fly. (n.d.). Retrieved from Real World Physics Problems: http://www.real-world-

    physics-problems.com/how-airplanes-fly.html

Lyon, C. A. (1997, December). *Summary of Low Speed Airfoil Data*. Retrieved from Illinois.edu:

    http://m-selig.ae.illinois.edu/uiuc_lsat/Low-Speed-Airfoil-Data-V3.pdf

Machinist Materials. (n.d.). Retrieved from Plastics Comparison Table: http://www.machinist-

    materials.com/comparison_table_for_plastics.htm

Pindado, S., Cubas, J., & and Sanz-Andres, A. (2013, December 4). *Aerodynamic Analysis of*

    Cup Anemometers Performance: The Stationary Harmonic Response. Retrieved from

    Scientific World Journal: http://www.ncbi.nlm.nih.gov/pmc/articles/PMC3868020/

Rogers, A. (2008, February/March). *Wind Power: Are Vertical Axis Wind Turbines Better?*

    Retrieved from Mother Earth News: http://www.motherearthnews.com/renewable-

    energy/vertical-axis-wind-turbines-zmaz08fmzmcc.aspx#axzz3Lcg3jwv7

63

Rumsey, C. (2014, June 23). *2D NACA 0012 Airfoil Validation Case*. Retrieved from NASA:

http://turbmodels.larc.nasa.gov/naca0012_val.html

The NACA Airfoil Series. (n.d.). Retrieved from Stanford.edu:

http://web.stanford.edu/~cantwell/AA200_Course_Material/The%20NACA%20airfoil%

20series.pdf

Turning Torque Calculation. (2014). Retrieved from ThyssenKrup Rothe Erde:

http://www.thyssenkrupp-rotheerde.com/gb/TG/Berechnung_des_Reibmomentes.shtm

Urban Green Energy Vertical Axis Wind Turbine. (n.d.). Retrieved from Solar Conduit:

https://solarconduit.com/shop/wind/urban-green-energy-vawt-uge5mc10m.html